THE JOURNAL OF COMPARATIVE NEUROLOGY 427:302–331 (2000)

Auditory Thalamocortical Projections in the Cat: Laminar and Areal Patterns of Input

CAMILLAN L. HUANG* AND JEFFERY A. WINER
Division of Neurobiology, Department of Molecular and Cell Biology, University of California at Berkeley, Berkeley, California 94720-3200

ABSTRACT

Thalamocortical projections were studied in adult cats using biotinylated dextran amines, wheat germ agglutinin conjugated to horseradish peroxidase, and autoradiography with tritiated leucine and/or proline. The input from 7 architectonically defined nuclei to 14 auditory cortical fields was characterized qualitatively and quantitatively. The principal results were that 1) every thalamic nucleus projected to more than 1 field (range, 4–14 fields; mean, 7 fields); 2) only the projection from the ventral division to some primary fields (primary auditory cortex and posterior auditory cortex) had a periodic, clustered distribution, whereas the input from other divisions to nonprimary areas was continuous; 3) layers III–V received >85% of the total axonal profiles; 4) in most experiments, five or more layers were labeled; 5) the projections to nonprimary auditory areas had many laterally oriented axons; 6) the heaviest input to layer I in all experiments was usually in its upper half, suggesting a sublaminar arrangement; 7) the largest axonal trunks (up to 6 μm in diameter) arose from the medial division and ended in layer Ia, where they ran laterally for long distances; 8) there were three projection patterns: type 1 had its peak in layers III–IV with little input to layer I, and it arose from the ventral division and the dorsal superficial, dorsal, and suprageniculate nuclei of the dorsal division; type 2 had heavy labeling in layer I and less in layers III–IV, arising from the dorsal division nuclei primarily, especially the caudal dorsal and deep dorsal nuclei; and type 3 was a trimodal concentration in layers I, III–IV, and VI that originated chiefly in the medial division and had the lowest density of labeling; and 9) the quantitative profiles with the three methods were very similar. The results suggest that the subdivisions of the auditory thalamus have consistent patterns of laminar distribution to different cortical areas, that an average of five or more layers receive significant input in a specific area, that a given thalamic nucleus can influence areas as far as 20 mm apart, that the first information to arrive at the cortex may reach layer I by virtue of the giant axons, and that several laminar patterns of auditory thalamocortical projection exist. The view that the auditory thalamus (and perhaps other thalamic nuclei) serves mainly a relay function underestimates its many modes for influencing the cortex on a laminar basis. J. Comp. Neurol. 427: 302–331, 2000.

Indexing terms: thalamus; neocortex; hearing; axons; forebrain; cortex

The current view of auditory thalamocortical connections recognizes at least two parallel pathways to the cortex, each with different implications for how the forebrain analyzes sound (Aitkin, 1990; citations refer to the cat unless noted otherwise). These streams have different laminar terminations (Niimi and Naito, 1974) in the cortex, arise from different populations of thalamic projection neurons (Mitani et al., 1987), and have unique functional contributions to sensory processing (Rose and Woolsey, 1949a; Winer, 1992). One pathway ends principally in layers III and IV (Wilson and Cragg, 1969) in primary

Grant sponsor: National Institutes of Health; Grant number: R01 DC02319-20.

Preliminary reports of these results have been previously published (Huang and Winer, 1997, 1998).

*Correspondence to: Dr. Camillan L. Huang, Division of Neurobiology, Room 285 Life Sciences Addition, Department of Molecular and Cell Biology, University of California at Berkeley, Berkeley, CA 94720-3200. E-mail: cammy@socrates.berkeley.edu

Received 24 March 2000; Revised 29 June 2000; Accepted 30 June 2000

auditory cortex (AI). This streamrepresents tonotopically organized information from narrowly tuned neurons that process the output of the prethalamic nuclei (Calford and Aitkin, 1983) with great fidelity (Aitkin, 1973) and convey it to the auditory cortex (Sousa-Pinto, 1973a) with topographic precision (Brandner and Redies, 1990) and at high speed (Clarey et al., 1992). A second stream arises from other thalamic nuclei (Rose and Woolsey, 1949b) and terminates primarily in layers I and VI in rodents (Patterson, 1976); its projections are more diffuse (Jones and Powell, 1973) and have less of a topographic organization (Rouiller et al., 1989), and they originate from much larger thalamocortical neurons (Mitani et al., 1987), possibly representing nonauditory as well as auditory peripheral information (Love and Scott, 1969). These differences suggest that the cellular targets of thalamocortical axons for the specific and the diffuse systems ought to be segregated, much as the retinal input to the lateral geniculate body has lamina-specific projection arrangements within the visual cortex (Humphrey et al., 1985) that also conserve their peripheral independence to some degree (Leventhal et al., 1981). These patterns of connectivity in the thalamocortical auditory system have been described using axonal degeneration in the cat (Sousa-Pinto, 1973a) and rat (Cipolloni and Keller, 1989) or autoradiographic methods (tree shrew: Oliver and Hall, 1978) and, more recently, with axonal transport or labeling in the rabbit (de Venecia and McMullen, 1994; Cetas et al., 1999) and primate (Hashikawa et al., 1995; Hackett et al., 1998). Although these techniques have revealed basic patterns of organization much like those in the thalamocortical visual system (Jones, 1984), all have technical limitations. For example, degeneration methods depend on the selection of an appropriate survival period and on the distinction between normal and pathological fibers (Morest, 1975b). Autoradiographic techniques provide little or no data on the structure of preterminal or terminal configurations of axonal endings (rat: Winer and Larue, 1987), nor do they reveal all connections with equal sensitivity or effectiveness within the auditory system (Sousa-Pinto and Reis, 1975). Neither method lends itself readily to a more rigorous, quantitative light microscopic approach to assess parallels and differences between thalamocortical pathways. Studies of axonal filling in the auditory system that address many of these concerns have considered mainly the projections from lemniscal nuclei and have concentrated on the rabbit (McMullen and de Venecia, 1993) and the monkey (Hashikawa et al., 1995), with far less attention to extralemniscal parts of the auditory thalamus or nonprimary cortical fields.

The present study reexamines the feline thalamocortical systems with a highly specific and sensitive tracer, biotinylated dextran amines (BDA; Brandt and Apkarian, 1992). The first goal was to delineate the areal and laminar termination patterns of presumptive axon terminals. This tracer reveals the structure of thalamocortical axons by filling them in a Golgi-like fashion to show their preterminal and terminal processes. We have corroborated the results with a second, equally sensitive and specific tracer, wheat germ agglutinin conjugated to horseradish peroxidase (WGA-HRP), following a strategy used in studies of corticocollicular projections (Winer et al., 1998). Other experiments used tritiated amino acids to explore and confirm these projections.

A second rationale for the present investigation is that the description of the laminar patterns now available with degeneration and axonal transport methods is confined largely to the cat primary auditory cortex (AI; Sousa-Pinto, 1973a; Niimi and Naito, 1974). Whereas a vast literature is available on the physiological properties of AI neurons (Aitkin, 1990; Clarey et al., 1992), far less is known about the arrangement of thalamocortical projections to the 13 other fields that, with AI, constitute the extended auditory cortex (Winer, 1992). The data are not yet available that would support the idea that the principles of specific laminar and focal, clustered input to AI from the auditory thalamus is conserved, especially for the nonprimary fields. Prior work used demonstrably less sensitive methods, such as autoradiography or axonal degeneration, than those now available. Moreover, thalamic

Abbreviations

A, A1, C	laminae of the lateral geniculate body
AAF	anterior auditory field
Abl	basolateral nucleus of the amygdala
Abm	basomedial nucleus of the amygdala
aes	anterior ectosylvian sulcus
AI	primary auditory cortex
AII	second auditory cortical area
Ala	lateral nucleus of the amygdala
Am	amygdala
BIC	brachium of the inferior colliculus
D	dorsal nucleus of the medial geniculate body
DCa	dorsal caudal division of the medial geniculate body
DD	deep dorsal nucleus of the medial geniculate body
DS	dorsal superficial nucleus of the medial geniculate body
EP	posterior ectosylvian gyrus
EPD	posterior ectosylvian gyrus, dorsal part
EPI	posterior ectosylvian gyrus, intermediate part
EPV	posterior ectosylvian gyrus, ventral part
GP	globus pallidus
Ins	insular cortex
LGB	lateral geniculate body
LP	lateral posterior nucleus
M	medial division of the medial geniculate body
MGB	medial geniculate body
MZ	marginal zone of the medial geniculate body
P	posterior auditory cortex
pes	posterior ectosylvian sulcus
Pr	piriform cortex
ps	pseudosylvian sulcus
R	rostral
RtN	thalamic reticular nucleus
SF	suprasylvian fringe auditory cortex (dorsal zone)
Sgl	suprageniculate nucleus, lateral part
TC	thalamocortical
Te	temporal cortex
V	lateral part of the ventral division of the medial geniculate body or ventral division of the medial geniculate body
Vb	ventrobasal complex
Ve	ventral auditory cortex
Vl	ventrolateral nucleus of the medial geniculate body
VP	ventral posterior auditory area
VPI	ventral posterolateral subdivision of the ventrobasal complex
VPm	ventral posteromedial subdivision of the ventrobasal complex
wm	white matter
I–VI	cortical layers

TABLE 1. Summary of Experiments

Area injected[1]	Experiment[2]	Tracer[3]	Volume/method	Survival (days)	Figures
V	1386L	10% BDA	Iontophoresis	7	1C, D, 2, 3
V	1392R	10% BDA	Iontophoresis	7	9A, 10A, 11A
V	997R	30% HRP	0.30 μl	2	12A, B
V	998R	30% HRP	0.10 μl	2	—
V	1081R	[^{3}H]leucine/proline	0.50 μl	4	14B
V	1081L	[^{3}H]leucine/proline	0.50 μl	4	—
V, D	998L	5% WGA-HRP	0.10 μl	2	—
V, D	1195R	5% WGA-HRP	0.15 μl	2	—
V, M, DD	1052R	5% WGA-HRP	0.10 μl	2	—
D	1403L	10% BDA	Iontophoresis	7	9E
DS, D	1384R	10% BDA	Iontophoresis	7	9C, 10A, 11A
DS, DD, Sgl	1413L	10% BDA	Iontophoresis	7	10B, 11B
DD	1413R	10% BDA	Iontophoresis	7	10B, 11B
DCa	1393L	10% BDA	Iontophoresis	7	1E, F, 4, 5, 10B, 11B
DCa	1393R	10% BDA	Iontophoresis	7	9B, 10B, 11B
DCa, D, V	1195L	5% WGA-HRP	0.15 μl	2	—
DCa, D, V	1197R	5% WGA-HRP	0.10 μl	2	12C, D
Sgl	1416L	10% BDA	Iontophoresis	7	9D
Sgl	1194L	5% WGA-HRP	0.15 μl	2	9D
Sgl	1197L	5% WGA-HRP	0.10 μl	2	—
Sgl, DD	1416R	10% BDA	Iontophoresis	7	10A, 11A
M	1407L	10% BDA	Iontophoresis	7	6, 7, 8, 10C, 11C
M	1407R	10% BDA	Iontophoresis	7	9F
M, DD	1392L	10% BDA	Iontophoresis	7	10C, 11C
M, Sgl	1194R	5% WGA-HRP	0.10 μl	2	—
M, Sgl	1198R	5% WGA-HRP	0.10 μl	2	12E, F
M, Sgl, DD	997L	30% HRP	0.25 μl	2	—

[1]V, ventral division of the medial geniculate body; D, dorsal division of the medial geniculate body; M, medial division of the medial geniculate body; DD, deep dorsal nucleus of the medial geniculate body; DS, dorsal superficial nucleus of the medial geniculate body; Sgl, suprageniculate nucleus, lateral part; DCa, dorsal caudal division of the medial geniculate body.
[2]L, left; R, right.
[3]BDA, biotinylated dextran amines; WGA-HRP, wheat germ agglutinin conjugated to horseradish peroxidase; [^{3}H]leucine, tritiated leucine.

nuclei and cortical areas now considered as auditory (Calford, 1983) were often omitted (Rose and Woolsey, 1949b), thus limiting the scope of the study.

We have reinvestigated the projections from each subdivision of the medial geniculate complex onto the many cortical fields now recognized as auditory. Along with the goals enumerated above, we analyzed axonal projections in each area quantitatively. Such data can reveal differences between laminar as well as areal patterns that the older methods could not. These differences could predict important functional consequences for the subsequent streams of intracortical processing that use the thalamocortical system as a hub. A final objective was to begin the analysis of the structure of auditory thalamocortical axons. Whereas several detailed descriptions of these fibers are available for primary visual cortex (primate: Blasdel and Lund, 1983), somatic sensory cortex (cat: Landry and Deschênes, 1981), and motor cortex (rat: Aumann et al., 1998) in several species (White and Keller, 1989), the auditory cortex has received far less attention. Analysis of the terminal plexus of thalamocortical axons will provide a basis for comparisons with other species and systems. Many facets of thalamocortical processing may be common to mammals. For example, thalamocortical neurons in different modalities strongly resemble one another morphologically (Ramón y Cajal, 1911); they likely use the same amino acidergic (glutamate or aspartate) neurotransmitter (Spreafico et al., 1992); they terminate in many of the same cortical layers (Jones, 1984); and their synaptic architecture is highly conserved (White and Keller, 1989). Most higher order visual (Woolsey, 1981b) and somatic sensory (Woolsey, 1981a) cortical representations have topographic organization of the peripheral sensory epithelium, but such maps are virtually absent in nonprimary auditory cortical areas (Woolsey, 1982). This suggests that nontopographic principles of organization in the auditory system remain to be described. Perhaps the nonprimary auditory thalamocortical projections preserve their topographic input, whereas their physiological arrangement is nontopographic. In either case, comparing primary and nonprimary areas may reveal basic principles of thalamocortical organization.

We found three types of auditory thalamocortical projection from a laminar perspective, and these patterns are both nucleus-specific and area-specific. Two types of spatial representation—clustered and continuous—were also recognized. These diverse patterns suggest areal, laminar, and nuclear specificity in thalamocortical relations.

Fig. 1. Auditory cortical subdivisions, summary of injection sites, and representative patterns of labeling. **A:** Anatomically and functionally defined fields (white lines) of auditory cortex subdivisions as depicted in prior physiological, connectional, or combined studies (AI, AII, AAF: Rose and Woolsey, 1949b; Andersen et al., 1980a; AAF, AI, P, VP: Reale and Imig, 1980; Imig and Morel, 1984; AAF, AI, P, VP: Morel and Imig, 1987; AI, P, VP: Bowman and Olson, 1988a,b; Ins: Clascá et al., 1997; SF: He and Hashikawa, 1998). These are projected schematically on a representative hemisphere. Squares indicate the location of photomicrographs C and E. **B:** Summary of thalamic deposits on schematic medial geniculate body sections at approximate percentages from the caudal tip expressed as decimals. Deposits represent 13 experiments using biotinylated dextran amine (BDA; black) and 3 experiments using wheat germ agglutinin conjugated to horseradish peroxidase (WGA-HRP; gray). Autoradiographic deposits are not shown. All nuclei except the ventrolateral nucleus of the dorsal division (Vl) were studied. Numbers refer to figures. **C–F:** Nissl preparations (C,E) of a radial cortical strip (area indicated in upper right corner) with matching BDA-labeled strip (D,F; origin and target in upper right corner). The input terminated in layers III/IV (D,F) with some in layer I (F). The ventral division (V) projection to primary auditory cortex (AI) was clustered (D, arrow), whereas the labeling from a caudal dorsal division (DCa) deposit to temporal cortex (Te) was continuous (D). **Insets:** Coronal section with the locus of the labeling in D,F. Planapochromat, N.A., 0.4, ×16.

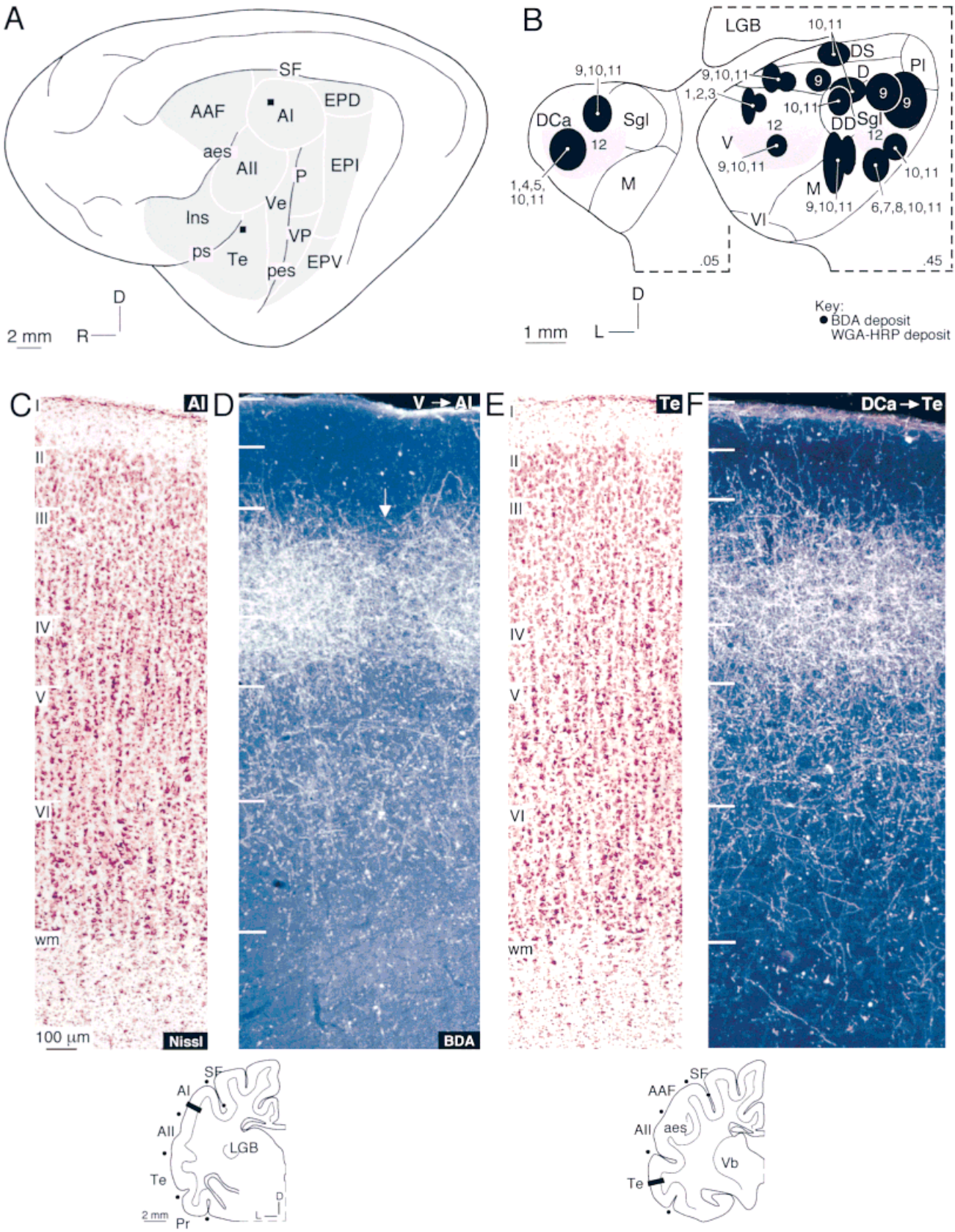
A
SF
AAF
AI
EPD
aes
AII
P
EPI
Ve
Ins
VP
ps
Te
pes
EPV
D
2 mm
R
B
LGB
10,11
DS
PI
9,10,11
9,10,11
D
9
1,2,3
9
9
10,11
DD
Sgl
12
DCa
Sgl
12
V
12
9,10,11
1,4,5,
10,11
M
M
9,10,11
6,7,8,10,11
10,11
VI
.05
.45
D
1 mm
L
Key:
BDA deposit
WGA-HRP deposit
C
AI
II
III
IV
V
VI
wm
100 µm
Nissl
D
V → AI
BDA
E
Te
II
III
IV
V
VI
wm
F
DCa → Te
SF
AI
AII
LGB
Te
2 mm
Pr
D
L
SF
AAF
AII
aes
Vb
Te

Figure 1

MATERIALS AND METHODS

Surgical procedures were approved by the local institutional animal care and use committee and were conducted under veterinary supervision. Preoperative and postoperative care followed extramural guidelines established by the National Institutes of Health and approved standard methods (Society for Neuroscience, 1991).

BDA was injected into the medial geniculate body of 13 hemispheres (Table 1) to bulk fill thalamocortical axons and terminals by diffusion (Brandt and Apkarian, 1992). In a parallel series of experiments, HRP or WGA-HRP was injected in 12 brains for purposes of replication and to confirm the BDA results independently. Perfusion and histological protocols in these studies followed standard methods (Mesulam, 1978). Tritiated proline/leucine was injected into two more hemispheres to allow for comparison of axoplasmic transport and bulk filling methods. These were also processed by a standard method (Cowan et al., 1972).

Surgery

Healthy adult cats of either sex, free of middle-ear disease, and weighing 2.6–4.8 kg were used. Anesthesia was induced with isoflurane (1–3%; Vetus) and adjusted to maintain stage III, plane ii of anesthesia; heart rate, blood pressure, electrocardiogram, respiration, and O_2 saturation were monitored continuously. Lactated Ringer's solution (50–150 ml, i.v.; 2-hour experiment) provided hydration, and a heating pad and drapes maintained body temperature (34–39°C). Postoperatively, a midrange dose of buprenorphine (0.00875 mg/kg) was given every 8–12 hours during the first 24 hours.

The animal was placed in a stereotaxic frame (David Kopf Instruments, Tujunga, CA), a midline cranial incision was made, the temporalis muscle and its attachments were blunt dissected, and a 5-mm-diameter craniotomy was made above the medial geniculate body. Coordinates were derived from a standard stereotaxic atlas (Berman, 1968) and adjusted to compensate for the size of the specimen. Iontophoretic deposits of 10% BDA (3 K molecular weight; Molecular Probes, Eugene, OR) in normal saline were made with glass pipettes (15–25 μm tip diameter) using a pulsed, positive, alternating current (7 seconds on/off, 5–6 μA for 20 minutes). Animals survived for 7–9 days, with 7 days being the optimal survival. Pressure injections of 30% HRP (type VI, P-8375; Sigma Chemical Company, St. Louis, MO) or 5% WGA-HRP (type VI, L-3892) were made with a 1-μl, 22-gauge microsyringe (Unimetrics Corporation, Shorewood, IL) at 0.05 μl per minute, with a total volume of 0.10–0.30 μl; animals survived for 48 hours. A more detailed protocol for the WGA-HRP experiments is available elsewhere (Mesulam, 1978; Winer and Larue, 1987).

Perfusion and histology

The cat was reanesthetized with sodium pentobarbital (26 mg/kg, i.v.), then perfused transcardially with wash out [0.12 M phosphate buffer (PB) and 0.001% lidocaine hydrochloride, 250 ml in a 3-minute wash] followed by fixative (2,000 ml 4% paraformaldehyde and 0.12 M PB, pH 7.4, for 20 minutes). Cryoprotectant (10% sucrose, PB, and 4% paraformaldehyde; 500 ml) was perfused 1 hour later. The brain was blocked stereotaxically, removed, and photographed before further cryoprotection (in 30% buffered sucrose and 4% formalin for 2–3 days). Frozen coronal sections 50 μm thick were cut and collected in alternating series for 3,5-diaminobenzidine (DAB) and Nissl or DAB/Nissl reactions. The DAB reaction was used for BDA localization (Adams, 1981). These sections were solubilized in 0.2–0.4% Triton X-100 for 20–25 minutes, incubated in HRP-avidin-biotin complex (ABC Elite reagent; Vector Laboratories; Burlingame, CA; double strength; 1 hour), and reacted with nickel/cobalt-enhanced DAB for visualization (20 minutes). Thorough rinsing between steps ensured low background levels. Both the DAB-reacted and unreacted sections (the latter reserved for Nissl staining) were postfixed (10% formalin and 2.5% glutaraldehyde for 10 minutes) and then fixed further (10% formalin and 0.1 M PB for 7–10 days) prior to Nissl staining. All sections were dehydrated in graded ethanols, cleared in xylenes, and coverslipped.

Data analysis. Thalamic and cortical cytoarchitectonic boundaries were drawn from Nissl preparations independent of the labeling. Anterogradely labeled axon terminals and retrogradely labeled neurons in DAB-reacted sections were plotted either through a drawing tube and/or Neurolucida™ image-analysis system (MicroBrightField Inc., Colchester, VT) with ×10–25 objectives for areal patterns and ×40–100 oil-immersion objectives for laminar analysis. The locus of the injection site and the terminal labeling patterns was determined by superimposing the adjacent Nissl-stained sections onto the DAB-reacted sections and aligning capillary profiles.

Areal distribution. Serial transverse sections of the labeling were aligned using prominent landmarks, superimposed, and projected onto a lateral view of the photographed hemisphere to create a three-dimensional view of the areal distribution pattern of thalamocortical projections. A case was accepted for analysis only when the deposit site and the ensuing anterograde labeling was confirmed in both BDA and WGA-HRP experiments.

Laminar analysis. Boutons (Fig. 13) were plotted from architectonically defined auditory fields with an oil-immersion objective (final magnification, ×940) through a drawing tube. Sample domains for within-laminae analyses were 50 μm wide (Fig. 3B) and extended radially from the pial surface to the white matter; for within-lamina studies (Fig. 3C), they were 150 μm thick and oriented tangentially. Laminar boundaries were drawn independently from the corresponding Nissl-stained section and were aligned with the labeled sections using blood vessels. The position of each bouton was measured from a digital

Fig. 2. Ventral division projections. **A:** Caudal-to-rostral extent of the deposit. **B:** Areal distribution from two ventral division deposits in the dorsal, midfrequency region as defined in physiological investigations (Imig and Morel, 1984); these labeled tonotopic areas AI, AAF, P, and Ve. Clusters of labeling were present in areas AI, P, and Ve. Thick dashed line indicates the location of C. Solid lines indicate the caudorostral loci of D–F. **C:** Plot of boutons in AI. **Inset:** Location of C. Five patches of labeling occur in layers III–IV. Dashed lines indicate the boundaries of Figure 3. **D:** Labeling in areas P (dorsally) and Ve was also focal. **E:** Five clusters of labeling crossed central AI. Deposits in other experiments in the midfrequency region of the ventral division (see Fig. 9A) also had patchy labeling. **F:** Clustered input in rostral AI; the middle band of labeling was heaviest. Protocol for Figures 2,4,6: Neurolucida™ plots. Subdivisions were drawn from adjacent, Nissl-stained sections Planapochromat; N.A., 0.7, ×250. For abbreviations, see list.

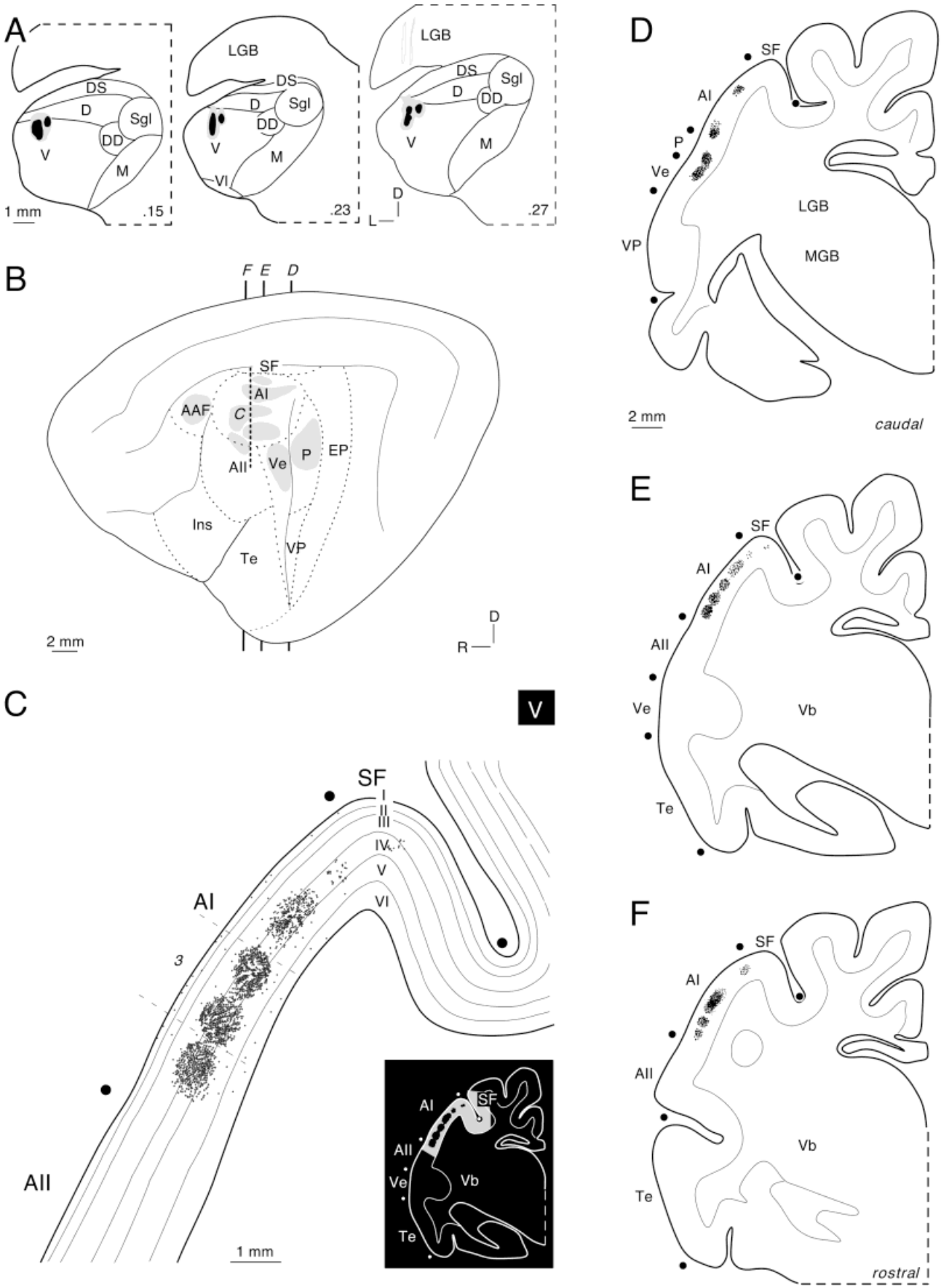
A
LGB
DS
D
Sgl
DD
V
M
VI
1 mm
.15
.23
.27
B
F E D
SF
AI
AAF
C
AII
Ve
P
EP
Ins
Te
VP
2 mm
D
R
C
V
SF
I
II
III
IV
V
VI
AI
3
AII
1 mm
D
SF
AI
P
Ve
LGB
VP
MGB
2 mm
caudal
E
SF
AI
AII
Ve
Vb
Te
F
SF
AI
AII
Vb
Te
rostral

Figure 2

image of the plot (NIH Image, version 1.61; National Institutes of Health, Bethesda, MD), and the number of boutons/layer was counted. Histograms (Figs. 10, 11) of laminar numerical density were made with standard software (Excel; Microsoft Corp., Redmond, WA) and analytic tools (S-PLUS; Mathsoft Inc., Seattle, WA). The histograms were analyzed to determine groupings and their structural relationships. Histograms were grouped together by cluster analysis (S-PLUS; Johnson, 1982). Histograms were then assigned to one of three categories based on the distribution of boutons per layer. A nonparametric analysis of variance was applied to evaluate the validity of the grouping into three patterns, and a bootstrap method (S-PLUS; Efron, 1993) was used to approximate the *P* value. We compared the within-group and the between-group variation using the Manhattan distance and analysis of variance as a measure of the difference between histograms. The null hypothesis was rejected ($P < 0.05$).

We wanted to explore the possibility of natural groupings in thalamocortical origin/target projection pairs. Each origin/target pair was represented as a histogram showing the number of boutons per layer. In preliminary studies, a cluster analysis was used to sort histograms along a dendrogram. Histograms were hierarchically clustered together based on their proximity, expressed as the distance between histograms. The Manhattan interval was chosen as the distance metric, because it is more suited for studying proportions in our example than the Euclidean distance. Histograms were converted mathematically into a six-dimensional vector with layers that represented one unit of the six-space vector, and the distance was based on these vectors. This strategy allowed us to apply multivariate statistics on the data for cluster analysis. No assumptions or hypotheses were made on the number of possible groups or structural relationships between them. Histograms with a common origin tended to be more tightly linked hierarchically. When we compared histograms with similar origins, we noticed that different thalamic nuclei had one of three different projection patterns. Thus, boutons were concentrated in layers III/IV (type I); in layers I and III/IV (type II); or in layers I, III/IV, and VI (type III). We tested the statistical validity of this categorical classification using a bootstrap analysis. A parametric model for the distribution of the six-dimensional vector could not be applied, so an alternative, nonparametric analysis of variance was used. The *P* value cannot be calculated from the standard formula, so a bootstrap method was used to compute the approximate *P* value. Thus, each of the three classes had unique and distinguishing features, and the grouping of our histograms by similar origins was neither subjective nor without empirical support.

RESULTS

Areal borders of the cortical fields (Figs. 1A,C,E, 9) were determined in Nissl preparations (Winer et al., 1998). Auditory thalamic subdivisions were related to Nissl sections from the experiments and with reference to Golgi and myeloarchitectonic studies in which the criteria for each subdivision have been enumerated (Winer, 1992). Three experiments illustrating the basic patterns are presented in detail (Figs. 2–7), whereas seven others are described briefly to confirm the main patterns (Fig. 9). All of the BDA deposits (Fig. 1B, black) and a few of the representative WGA-HRP injections (Fig. 1B, gray) are shown for comparative purposes on medial geniculate body sections representing the approximate caudorostral locus of injection.

Projections of the ventral division

The major features of ventral division neurons are reviewed here as a prelude to the experimental results. They are critical for accurate sound localization (Neff et al., 1975), have a stereotyped morphology in several species (Winer and Wenstrup, 1994), receive topographic projections from the midbrain (Andersen et al., 1980b), respond exclusively to auditory stimuli (Aitkin, 1976), and have narrow physiological tuning curves (Aitkin et al., 1981). They differ from dorsal and medial division cells in that they have a specific laminar arrangement (Morest, 1964), fewer sources of ascending input (Calford and Aitkin, 1983), shorter latencies to peripheral input (Aitkin and Webster, 1972; Aitkin, 1973), and a more focal set of cortical projections (Niimi and Matsuoka, 1979).

The two parallel pipette penetrations traversed the optic tract (Fig. 2A, .27) and ended in the caudal one-sixth of the medial geniculate body at the border of the ventral division and the dorsal nucleus (Fig. 2A, .15). The effective injection site was ≈1 mm in diameter (Fig. 2A, black), with two foci separated by <200 μm. The surrounding zone of diffusion (Fig. 2A, gray) did not contribute to the projection, because no neurons in it were labeled, nor were axons traversing this region likely to have been damaged. The deposits were centered in the lateral one-third of the ventral division, where physiological studies suggest that frequencies of ≈4–8 kHz are represented (Imig and Morel, 1985).

The ensuing anterograde labeling (Fig. 2B, gray) formed eight discontinuous patches that spanned >15 mm of cortex. All of the projections were confined to architectonically defined fields of primary and adjoining auditory cortex [Fig. 2B: AI, anterior auditory field (AAF), ventral auditory cortex (Ve), and posterior auditory cortex (P)]. Three features of the ventral division experiments distinguished them from other cases. They alone had a patchy, clustered distribution of terminal labeling. The density of the bouton-like, punctate structures, which are believed to represent axonal swellings, waxed and waned in horizontal traverses (Fig. 3C). Numerically, the bouton density for ventral division deposits was substantially higher than that for the dorsal division (59% of the ventral division value; Fig. 5C) or for the medal division (8.6% of the ventral division value; Fig. 7C). In vertical traverses through cortical areas with the heaviest labeling in an experiment (Figs. 3B, 5B, 7B), these relative proportions were preserved. This suggests that, along with the areal and laminar differences among the thalamocortical projections, functionally distinct patterns of input may also occur. A second theme common to all experiments was that at least three cortical layers were involved in the projection, and sometimes all six were labeled. In general, the ventral division experiments had a more distinct peak in layer III than the other deposits (Fig. 11A, 1). Finally, the ventral division experiments were unique in labeling the fewest cortical areas of the seven subdivisions of the auditory thalamus included here (Table 2).

Clusters of terminal labeling were present in transverse sections, where four or five foci were present through AI

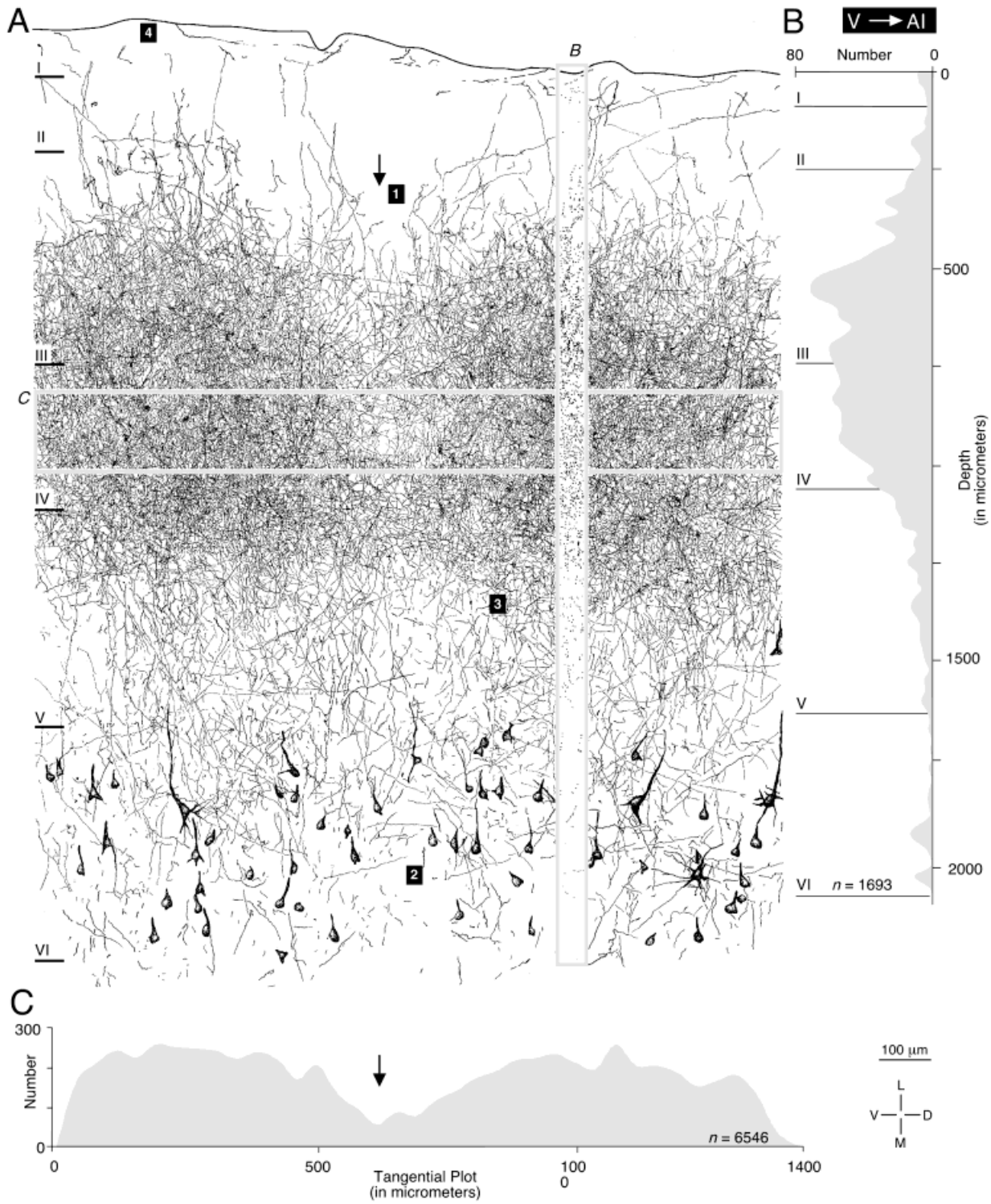

Fig. 3. Thalamocortical axons in AI from ventral division deposits (see Fig. 2). **A:** Axons formed clusters separated by zones of lighter labeling: 1: Labeling was intense from lower layer III to upper layer V (3; arrow; see also C). Clusters were ≈600 μm wide; the lighter zone of labeling also had fewer corticothalamic cells and was ≈150 μm wide (2). The clusters may be part of the binaural system in AI demonstrated physiologically (Imig and Adrián, 1977; Middlebrooks and Zook, 1983). Input to layer I (4) was sparse and consisted mainly of horizontal fibers. Laminar (gray column) and intralaminar (gray band) bouton plots were analyzed quantitatively (B,C; see also Figs. 10, 11). Planapochromat; N.A., 1.32, ×1,250. **B:** Laminar distribution of axon terminals. Input was centered in layers IIIb and IV, similar to the ventral division projection in other species (monkey AI: Hashikawa et al., 1995). Protocol: All boutons in a 50-μm-wide strip were plotted at 25-μm intervals. Planapochromat, N.A., 1.32, ×1,250. Boutons were digitized (NIH Image, version 1.61; National Institutes of Health, Bethesda, MD) and counted. Layers were drawn in adjacent Nissl preparations. Software packages were used for analyses (Excel; Microsoft Corp., Redmond, WA; S-PLUS: Mathsoft Inc., Seattle, WA). **C:** Quantitative analysis of the tangential distribution. Peaks of dense labeling were separated by a trough (arrow) less than one-third the value of the peaks. For protocol, see B, except that the strip was 150 μm wide, and data were collected along the tangential plane (rectangle in A). AI, primary auditory cortex; I–VI, cortical layers; D, dorsal plane of section; L, lateral plane or section; M, medial plane of section; V, ventral plane of section.

(Fig. 2D–F). The intercluster regions were also labeled (Fig. 2C) but at a value less than half of that seen in the center cluster (Fig. 3C, arrow). Labeling near the AI and the suprasylvian fringe (SF) border was conspicuously lighter (Fig. 2E), whereas the ventralmost clusters, near the border with the second auditory cortex (AII; Fig. 2E), were intense. Input to the posterior (P) and ventral (Ve) fields was equally strong and clustered (Fig. 2D). The projection to adjoining fields was sparse or absent (Fig. 2F).

At higher magnification, the terminal plexus of thalamocortical axons formed a dense matrix, with periodic discontinuities in labeling density (Fig. 3A, arrows). Punctate structures were present in every cortical layer (Fig. 3B), with >80% in layers III–IV (Figs. 10A, 11A). The projection to the upper half of layer III was far less than that to layer IIIb, suggesting a sublaminar organization of input congruent with the cytoarchitecture and neuronal architecture of layer III (Winer, 1984b,c). Even layer V, which is not usually considered as a specific target of thalamocortical input (Jones, 1985), had a few punctate structures, as did layer II, which likewise is regarded as devoid of such projections. Because the preterminal axons ascending to layers I–IV must traverse layer V, it implies that these boutons are not misplaced from their actual target and represent actual, albeit minute, projections. The massive concentration of ventral division boutons in layer III and their virtual absence in layer I (Fig. 3A) distinguished this pattern from that following deposits in the dorsal or medial divisions (Fig. 11C, 5, stippled area). Interestingly, the few layer I boutons were in layer Ia; in none of the experiments was there a significant projection to layer Ib (Fig. 10, I). Similar quantitative and laminar patterns in AI were noted with other tracers (Fig. 14). The matching corticogeniculate reciprocal projection was robust in layer VI, where a few thalamocortical boutons were seen (<0.5% of the total; Fig. 3A, stippled profiles; Fig. 11A) scattered among corticofugal neurons.

Projections of dorsal division nuclei

Dorsal division neurons contrast with those of the ventral division in almost every particular (Winer, 1992). They have a more diverse neuronal architecture (Winer and Morest, 1983a,b, 1984), a different set of midbrain (Calford and Aitkin, 1983) and corticothalamic (Diamond et al., 1969) connections, and a physiological organization dominated by broad tuning curves and a limited degree of tonotopic organization (Aitkin and Prain, 1974). In contrast, the ventral division is exclusively auditory, whereas the medial division has extensive polymodal affiliations (Wepsic, 1966) and an integrative role in sensory perception (Winer and Morest, 1983a).

To capture the range of dorsal division cortical areal (Table 2) and laminar (Fig. 10B) projections, five representative nuclei were chosen, including the dorsal superficial (DS), dorsal (D), deep dorsal (DD), caudal dorsal (DCa), and suprageniculate (Sg) nuclei. The principal features that distinguished the dorsal division thalamocortical projection from the ventral division pattern were 1) the primary (tonotopically organized) auditory fields received a much smaller input than the nonprimary (nontonotopic) fields; 2) the heaviest projections were to nonprimary areas in the posterior ectosylvian region and in the insular and temporal cortex; 3) the laminar distribution of thalamocortical afferents was grossly similar to that of the primary fields, except that the projection from the DCa and DD nuclei always involved layer I more extensively than did the latter; 4) whereas layers III–IV in nonprimary cortex were the main targets of dorsal division projections (Fig. 10B, 2–4 and 6–8), there was less labeling in them than in the primary areas (Fig. 10A, 1–12); and 5) the dorsal division thalamocortical projection had a more extensive lateral, laminar distribution, and it was never clustered or periodic like that of the ventral division.

In a representative experiment, the deposit involved only the DCa nucleus, which forms the posterolateral pole of the medial geniculate body (Winer, 1985a), and it did not extend beyond this nucleus (Fig. 1A; Table 1). The deposit was 1 mm tall, 1.5 mm wide, and had an anteroposterior span of ≈500 μm with a light halo of diffusion.

The anterograde labeling targeted mainly nonprimary areas along the lateral perimeter of the hemisphere. Altogether, nine fields were involved, and the broad range of fields labeled by dorsal division deposits (n = 4–9; Table 2) argues that the degree of cortical divergence for each thalamic nucleus is somewhat different; only medial division deposits had a wider distribution (Figs. 6, 10). Three primary areas along the posterior ectosylvian sulcus were involved [Fig. 4B: P, Ve, and ventral posterior auditory area (VP)]. The most salient qualitative feature of the projection was its areal and laminar continuity. More than half of the cortical areas labeled were contiguous, and the other regions were <2 mm away except for the perirhinal cortex [Fig. 4B: piriform cortex (Pr)]. The laminar continuity was conserved across distances of 10 mm or more, where clusters or discrete patches of labeling were entirely absent (Fig. 4C). Along with the laminar breadth of dorsal division deposits (compare Fig. 10A, 2 with Fig. 10B, 2), two other features were noteworthy. First, the deposits in DCa labeled up to about five times as many terminals per injection than those in the ventral division (compare Fig. 10A, 6 with Fig. 10B, 2). Only one other projection, which also arose from the dorsal division (Fig. 10A, 11), had more than half as many boutons. Second, the labeling in the different layers overlapped spatially (Fig. 4C, dots), except in parts of the perirhinal (Pr; Fig. 4D) and temporal (Te; Fig. 4E) cortices. Labeling density across layers III and IV was uniform (Fig. 4C), although there was variability near architectonic borders (Fig. 4F; junction of the insular [Ins] and Te cortices). The patterns noted above, including the areal distribution, were confirmed in other experiments (Fig. 9B).

The laminar distribution of boutons (Fig. 11B) arising from the dorsal division was distinct from the ventral division projection (Fig. 11A). In the latter, only 6 of 12 samples from primary auditory areas had any layer I input, and the largest such projection was comprised of 3.7% of the total number of boutons in the experiment (Fig. 11A, 9). In contrast, all seven cortical samples involving the DCa nucleus and its related nuclei had such a layer I projection, and these ranged from 5.5% to 15.9% of the total number of boutons (Fig. 11B, 1–4 and 6–8). Analysis of laminar (Fig. 5C) and interlaminar (Fig. 5B) projections confirmed these observations and revealed that every layer in area Te received some puncta, that their distribution was nonuniform within most layers and was concentrated preferentially in one half (save for layer II), and that the density of preterminal fibers was correlated highly with the bouton density.

The labeling from caudal dorsal nucleus injections was largely continuous except for 200–300-μm-wide, puncta-free expanses (Fig. 5A, 1) that, unlike the clusters in the primary fields (Fig. 3A, arrows), were smaller, had no discernible periodic distribution, and were less regular. Ascending axons entered layer VI and ramified obliquely, converging mainly in layers IV, III, and I. Many preterminal and bouton-bearing fibers in layers IV and III were oriented vertically, whereas a significant proportion had a horizontal configuration that was tangential and fasciculated. There was a marked sublaminar distribution within layer I—with >90% of the boutons in layer Ia—and the tangential fibers were neither fasciculated nor clustered. Corticogeniculate reciprocal projections were rare in some experiments (Fig. 5A) despite appreciable thalamocortical input. Such interexperimental differences suggest that there may be an area-specific corticothalamic contribution and that the intracortical axons of corticothalamic neurons—fibers that could rarely be traced to their parent cells of origin—contributed few if any branches that might be confounded with thalamocortical auditory fibers. The results also confirm that significant regions of corticogeniculate nonreciprocity complement the analogous zones of such nonreciprocity in the medial geniculate body (Colwell, 1975).

Projections of the medial division

Medial division neurons contrast with ventral or dorsal division cells in almost every particular. The medial division has many resident cell types but no nuclear subdivisions in cats (Winer and Morest, 1983a), little topographic input from the brainstem (Calford and Aitkin, 1983), a much smaller overall proportion of neurons that are immunopositive for γ-aminobutyric acid (GABA; Huang et al., 1999), only a coarse tonotopic arrangement (Rouiller et al., 1989), and significant projections to nonauditory cortex (Jones and Powell, 1973) and to the amygdala (Shinonaga et al., 1994).

The principal features of the medial division thalamocortical projection likewise distinguish it from the ventral and dorsal division patterns. These include the involvement of many cortical layers (all layers in 5 of 7 samples; Fig. 11C, 1–4 and 6–8), a far lower overall puncta density average in each projection (Fig. 10), and a laminar distribution in which layers III and IV were labeled as heavily or more heavily than layers I and VI (5 of 7 experiments; Fig. 11C, 1–4 and 6–8). Finally, the largest caliber thalamocortical axons arise from medial division neurons and terminate in layer I.

A representative deposit traversed the dorsal superficial and suprageniculate nuclei (Fig. 6A, .26) and was centered in the medial division, filling ≈1 mm^3 with minor diffusion into adjoining nuclei. The ensuing labeling occupied ≈300 mm^2 of auditory cortex (Fig. 6B) and involved all 14 areas considered here as auditory (Table 2) but spared the second somatic sensory area (SII) and adjoining fields, which had significant degeneration or transport in other studies of medial division cortical connectivity (Jones and Powell, 1973). The labeling was neither as clustered as that in the ventral division experiments (Figs. 2, 9A) nor as continuous within layers as that from dorsal division experiments (Figs. 4D–F, 5). The projection consisted of diffuse patches of heavier input linked by sparsely labeled regions (Fig. 6C, III). Labeling in one layer within an area (Fig. 6C) was usually accompanied by labeling in other layers, except near areal borders (Fig. 6E, AII-Ve junction). Within a field, the labeling ranged from clustered and patchy (Fig. 6F, Ins) to more regular (Fig. 6E, Ins). Specific medial division subregions did not invariably project to all subdivisions of auditory cortex in each experiment (Fig. 9F), implying that there is a spatial threshold for thalamocortical connectivity that the smallest deposits do not reach or that a subpopulation of medial division axons is too fine to be labeled with BDA; these issues are considered further below (see Discussion).

The laminar distribution of medial division axons was as distinct as the areal pattern, involving an average of 5.4 layers (Fig. 11C) and contrasting with the smaller values in the ventral (4.6) and dorsal (4.7) divisions, respectively (see also Figs. 14, 15A). Despite the laminar breadth, the overall density of medial division labeling was far lower than that from the ventral and dorsal divisions (Fig. 10). Although many prior investigations have emphasized the medial division terminations in layers I and VI (Table 4), in the present study, these boutons represented only 42% of the total (n = 8), the same numerical values found in layers III and IV in this material (Table 3). Moreover, the layer II contribution (27% of the total) was the third highest in this sample (n = 18), despite qualitative density differences in intensity (compare Fig. 12A with Fig. 12C). This laminar pattern has been designated type 3 (Fig. 11C, 5). Traverses of single fields confirmed these impressions, with peaks in layers I,VI, III, and IV. The projection to layer I always involved the superficial half, with few boutons in layer Ib in this and the other experiments (Figs. 3A, 5A, 7A). Although the mediolateral concentration of labeling was continuous (Fig. 7C), the periodic fluctuations were sharper and more finely grained than those from ventral division (Fig. 3C) or dorsal division (Fig. 5C) deposits. The relative comparability of the deposits in size and shape (Fig. 9, insets) and the uniform survivals (Table 1) suggest that internuclear differences in projection are not an artifact of method.

Two other facets of the medial division projection are relevant. First, these fibers have a prominent lateral component in other layers outside of layer I. Although a representative sample may show only a few tangential fibers in layers II–VI (Fig. 7A), these axons are certainly numerous enough to form a prominent component in layers III, IV, and VI (Fig. 8C,D,F), especially if the medial division projection in its entirety were to be considered. A second feature was that the thickest caliber fibers by far—up to 6 μm in diameter (Fig. 8A, 1) and about twice the diameter

Fig. 4 (Overleaf). Cortical connections of the caudal dorsal division. **A:** The injection was ≈1 mm in diameter and was confined to the caudal tip of the medial geniculate body. **B:** The ensuing labeling lay in tonotopic (P, VP, Ve) and nontonotopic (AII, Ins, Te, Pr) areas. Thick dashed line through Te shows the locus of C. **C:** Temporal cortex labeling showing approximate bouton densities. The heaviest labeling was in layers I and IIIb/IV. **Inset:** Locus of labeling; dashed lines indicate the locus of Figure 5. **D:** Caudal-to-rostral sections (D–F) through the labeling. A continuous input extended across the midcortical layers in the ventral field (Ve) with a thinner band in the ventral posterior (VP) auditory area. The lamination in Ve was distorted by the posterior ectosylvian sulcus. Layer I labeling was present in both areas. **E:** The heaviest and most extensive AII and Te labeling was in layers I and III–IV. **F:** Dense labeling extended to the rostralmost part of Te. For protocol, see Figure 2.

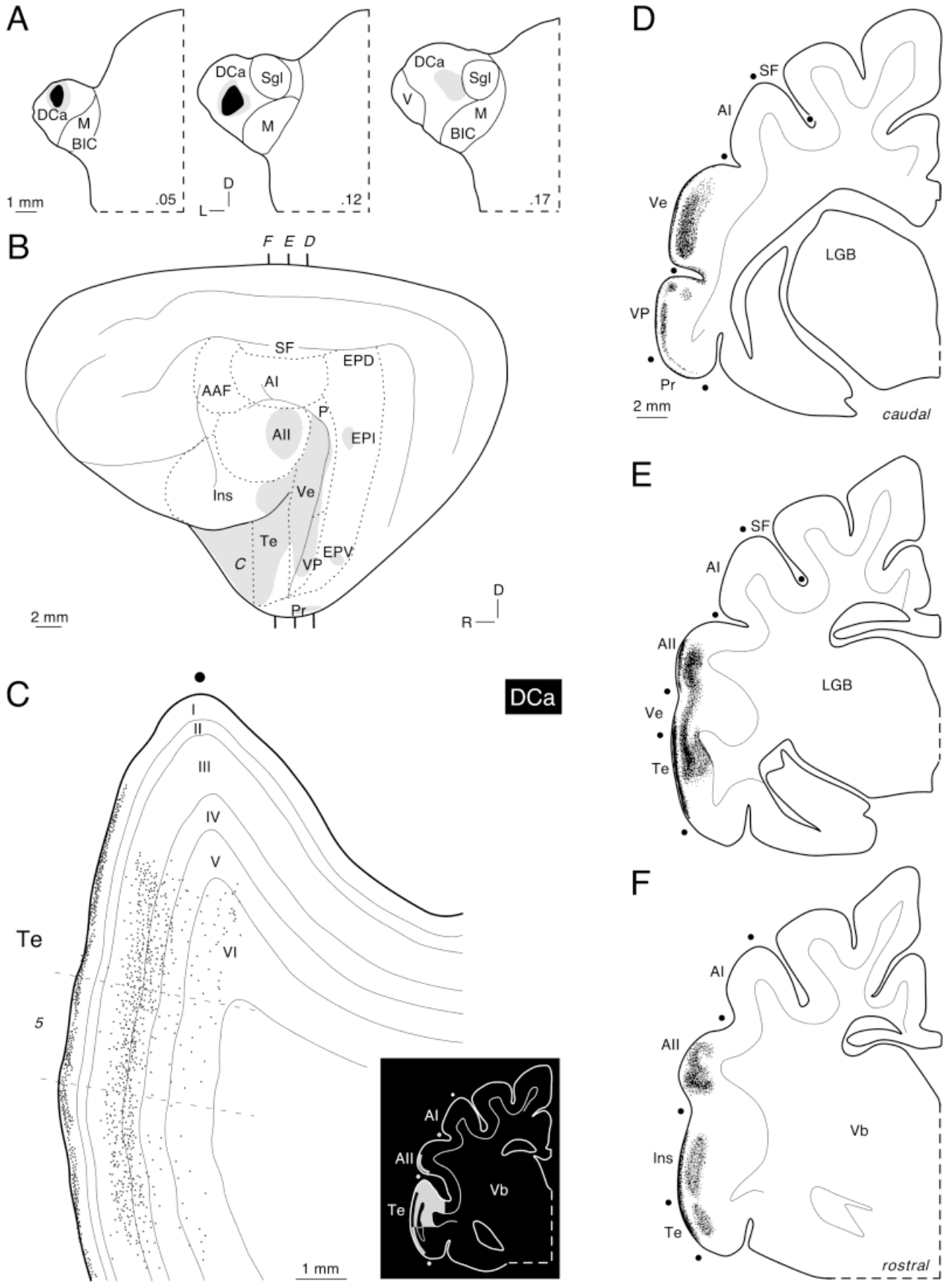

Figure 4 (Overleaf)

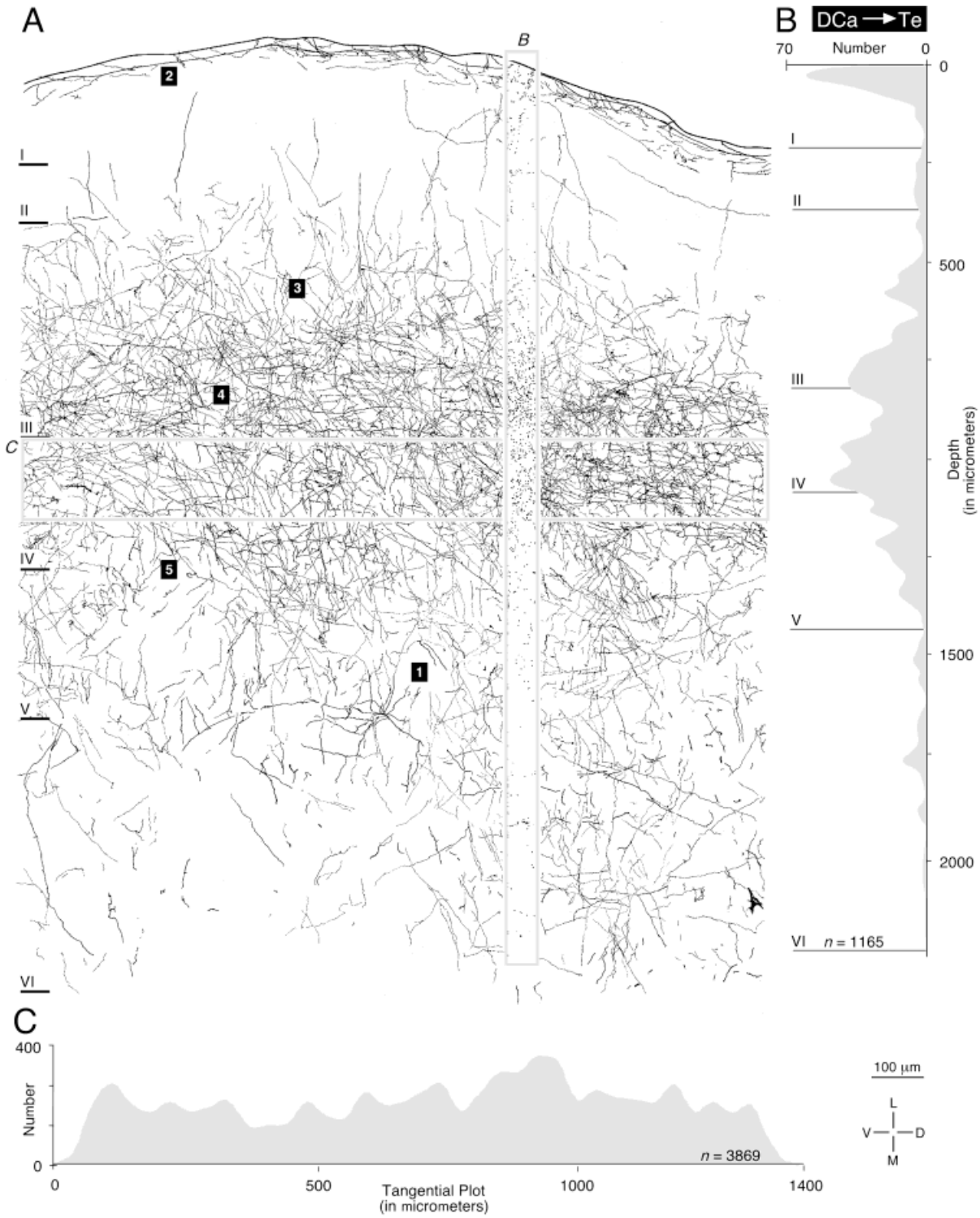

Fig. 5. Laminar distribution of thalamocortical axons in the temporal cortex (Te) from a caudal dorsal division deposit (Fig. 4). **A:** Labeling in Te was continuous (1). Horizontal axons were more apparent in layers IIIb–IVa (4) in Te than in area AI after a ventral division deposit (compare with Fig. 3A). Layer IIIa, however, had more vertically oriented axons (3). There was a significant input to layer Ia in contrast to AI (2; Fig. 3A). Boutons were found in all layers, as in AI, with a significant input to layer V (5). Fewer layer VI corticothalamic neurons were found in Te than in AI experiments, suggesting a lack of complete corticothalamic reciprocity. Gray band and column represent sample domains (B,C). **B:** The laminar distribution had peaks in layers I, III, and IV. Layer I labeling was heavier than that in layers III or IV. **C:** The lateral distribution of labeling across Te in layer IV (stippled vertical rectangle) was homogeneous relative to the patchiness in AI (compare with Fig. 3C). For protocol, see Figure 3. DCa, dorsal caudal division of the medial geniculate body.

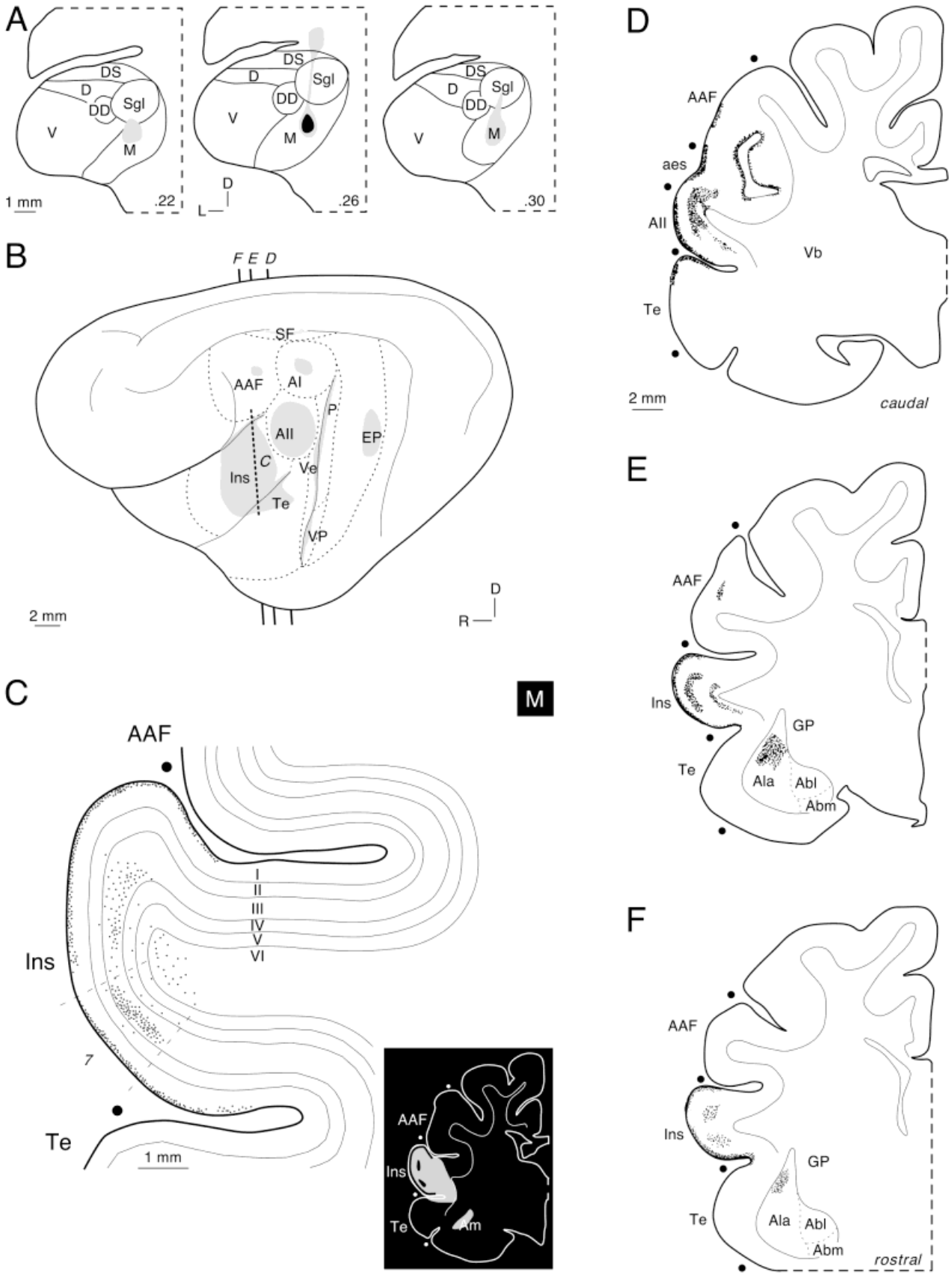

Fig. 6 Cortical projection of the medial division. **A:** This deposit encroached slightly into the suprageniculate nucleus (Sgl) and labeled every auditory field diffusely. **B:** Thick dashed line through insular cortex (Ins) shows the locus of C. **C:** Laminar distribution of boutons. Most of the labeling lies in layers I, III, IV, and VI. **D:** Representative coronal sections appear in D–F. Labeling was most prominent in layer I of insular cortex (Ins) and along the caudal bank of the anterior ectosylvian sulcus. **E,F:** Projections were continuous and focal in caudal Ins and discontinuous in rostral Ins. The projection to the amygdala (documented in Shinonaga et al., 1994) consisted primarily of fine, beaded axons (not illustrated).

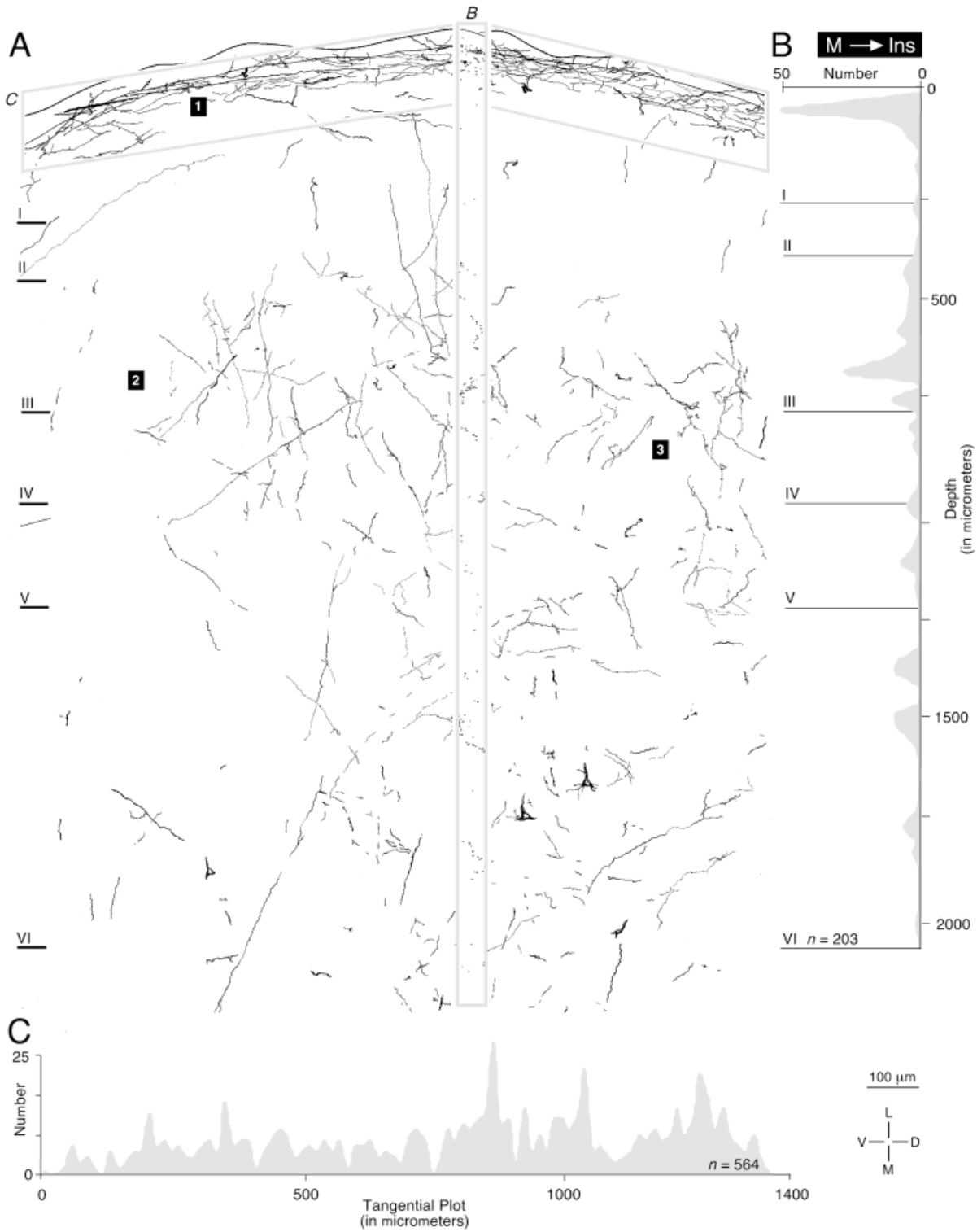

Fig. 7. Laminar distribution of medial division (M) axons in insular cortex (Ins) (deposit site shown in Fig. 6). **A:** This injection (see Fig. 6A) produced a more diffuse labeling pattern in Ins than in AI or Te (compare with Figs. 3A, 5A). There were many horizontal axons in layer Ia (1). Labeling to layer III was lighter than to AI or Te (compare with Figs. 3A, 5A) with axons that were more oblique (2) or sinuous and had clasp-like endings (3). **B:** The laminar distribution plot showed labeling peaks in layers I and III–IV and smaller puffs of transport in layer VI. The principal targets in Ins are layer I and VI, in agreement with prior work (Sousa-Pinto, 1973a; Mitani et al., 1984). This projection, in contrast to that in AI and Te, was more diffuse (compare Figs. 3B, 5B). **C:** Labeling across Ins was continuous, like that in Te (Fig. 5C) and other areas (not shown), in comparison to the clustering in AI (compare with Fig. 3C). For details of the protocol, see Figure 3.

TABLE 2. Auditory Cortical Targets of the Cat Medial Geniculate Body

	Cortical area[1]													
	Tonotopic						Nontonotopic							
MGB	AI	AAF	P	VP	Ve	AII	EPD	EPI	EPV	Ins	Te	SF	AES	Pr
Subdivision[2]														
V	●	●	●		●									
DS	•		●	●	●	●		●	•			●		
D	•					●		●	●			●	●	
DD		•				●				●	●		●	●
DCa			•	●	●	●		•	•	●	●			●
Sgl							●	•		●		●	●	
M	●	●	●	●	●	●	•	●	●	●	●	●	●	●

[1]MGB, medial geniculate body; AI, primary auditory cortex; AAF, anterior auditory field; P, posterior auditory cortex; VP, ventral posterior auditory area; Ve, ventral auditory cortex; AII, second auditory cortical area; EPD, posterior ectosylvian gyrus, dorsal part; EPI, posterior ectosylvian gyrus, intermediate part; Ins, insular cortex; Te, temporal cortex; SF, suprasylvian fringe auditory cortex (dorsal zone); AES, anterior ectosylvian field; Pr, piriform cortex; ●, heavy; ●, moderate; •, light.
[2]Subdivisions of the MGB: V, ventral; DS, dorsal superficial; D, dorsal; DD, deep dorsal; DCa, caudal dorsal; Sgl, suprageniculate; M, medial.

TABLE 3. Quantitative Laminar Analysis of Auditory Thalamocortical Projection Patterns

	Layer						No. (df)[1]
Type	I	II	III	IV	V	VI	
Percentage of boutons ± S.D./layer							
Type 1	2 ± 2	4 ± 4	58 ± 25	20 ± 12	12 ± 13	4 ± 5	n = 21
Type 2	10 ± 4	2 ± 2	42 ± 16	25 ± 11	17 ± 7	4 ± 3	n = 12
Type 3	25 ± 18	3 ± 3	29 ± 19	17 ± 8	5 ± 3	21 ± 12	n = 8
Intralaminar statistical comparisons (*P* values)							
Type 1 = Type 2?	0.001	0.05	0.05	—	—	—	(16)
Type 1 = Type 3?	0.01	—	0.01	0.05	—	0.01	(7)
Type 2 = Type 3?	—	—	—	0.05	0.001	0.01	(7)

[1]Number of samples: The degrees of freedom (df) are shown in parentheses.

of other thalamocortical axons (Fig. 8C)—were a singular feature of auditory thalamic input to layer I from the medial division. The massive trunks extend for 250–300 μm across layer Ia, emitting collaterals at right angles as they traverse the neuropil or doubling back to form corkscrews (Fig. 8A, 3) before ending in terminal sprays across the depth of layer Ia (Fig. 8A, 2). The preterminal trunks had few boutons.

DISCUSSION

The appropriateness and resolution of the techniques used to demonstrate the auditory thalamocortical projections are evaluated first. The laminar patterns of auditory thalamocortical projection are then contrasted and compared with one another and with those in other modalities. Finally, the implications of the findings for cortical processing are considered.

Methodological considerations

The primary datum in this study is the density and distribution of experimentally labeled round, oval, or oblate profiles ≈0.5–2.0 μm in diameter and associated with ascending axons that can often be traced into the white matter. It is unknown whether these profiles are plausibly synaptic or merely represent nonsynaptic axonal dilatations. Their synaptic identity is likewise unknown, because that would require electron microscopic analyses beyond the scope of this study. Ultrastructural (rat: LeVay and Gilbert, 1976; Peters and Feldman, 1977) and high-resolution light microscopic studies in the visual (Humphrey et al., 1985) and somatic sensory cortex (Jones and Powell, 1970) found that the experimentally labeled or degenerating thalamocortical presynaptic processes closely resemble those profiles labeled here by diffusion and/or active transport (Brandt and Apkarian, 1992). The dimensions and shapes of thalamocortical synaptic boutons in other modalities closely match those of the light microscopically characterized profiles in the present study. Further parallels are that many types of thalamocortical neurons in the auditory (Morest, 1975a), visual (Guillery, 1966), and somatic sensory (Scheibel and Scheibel, 1966) thalamus resemble one another morphologically (the so-called *Buschzellen*; Jones, 1985). In the corresponding nucleus for each modality, these neurons have processes of similar size (Morest, 1964, 1965; Friedlander et al., 1980; rat: McAllister and Wells, 1981), their axons project to matching cortical layers (Leventhal, 1979; Niimi et al., 1984; rat: Jensen and Killackey, 1987; Fig. 13), and they may be glutamatergic (rat: Popowits et al., 1988; Uhlrich and Huguenard, 1995; Salt and Eaton, 1996).

The present results cannot be used to predict the synaptic affiliations of any presumptive terminal (rat: Markram et al., 1998). At best, they represent population estimates of the relative density and laminar disposition of auditory thalamic input to a layer or sublayer. As a case in point, the sparse projection to layer II shown here (Table 4) may not represent an input; nevertheless, the inconsistency of axonal degeneration (Wilson and Cragg, 1969) and of autoradiographic studies (Sousa-Pinto and Reis, 1975) suggests that such fine projections may transcend the resolution of older methods.

Our study used labeled puncta as the primary dependent variable for quantitative purposes. Because this is one of the first investigations to use such structures for light microscopic analysis of the strength of connectivity,

TABLE 4. Comparison of the Laminar Distribution of Thalamic Projections to Sensory Cortex Using Anterograde Methods

Reference and species	Method[1]	Layer[2] I Ia	I Ib	II	III IIIa	III IIIb	IV IVa	IV IVb	V Va	V Vb	VI VIa	VI VIb	Patches?	Nuclear subdivision[3]
Auditory thalamus														
Medial geniculate body (cat)														
Wilson and Cragg (1969)	Nauta	●	●	●	●	●	●	●	●	●	●	●		
Sousa-Pinto (1973a)	Wiitanen	•			●	●	●	●	●	●	●	●		
Niimi and Naito (1974)	Nauta	•			•	●	●	●	•	•	•	•		
Shinonaga et al. (1994)	PHA-L	●			•	●	●	●	•	•	•	•		Dorsal, M
Present results	BDA, WGA-HRP [3H]leucine, proline													
Type 1		•		•	●	●	●	●	●	•	•	•	AI	V, Sgl, D, DS
Type 2		●		•	●	●	●	●	●	•	•	•		DCa, DD
Type 3		●		•	●	●	●	•	•	•	●	●		M
Other species														
Ryugo and Killackey (1974; rat)	Fink-Heimer	•	•		●	●	●	●						
McMullen and de Venecia (1993; rabbit)	Biocytin	●	●		●	●	●	●					AI	
Oliver and Hall (1978; tree shrew)	Fink-Heimer, [3H]leucine													
Pattern 1						●	●	●	•	•	•	•		V
Pattern 2		•				●	●	●		•	●	●		DCa, M
Mesulam and Pandya (1973; monkey)	Fink-Heimer, Nauta					●	●	●	●					
Hashikawa et al. (1995; monkey)	WGA-HRP, PHA-L												AI	V
Pattern 1		•	•	•	•	●	●	●			•	•		
Pattern 2		●	●	•	•	●	●				●	●		M
Visual thalamus														
Lateral geniculate body (cat)														
LeVay and Gilbert (1976)	[3H]proline													
Pattern 1						•	●	●			●	●		A, Al laminae
Pattern 2		●				●	●	●	●					C lamina
Ferster and LeVay (1978)	HRP into optic tract					●	●	●			●			
Humphrey et al. (1985a,b)	HRP, intraaxonal					●	●	●			●			A, Al laminae
Other species														
Peters and Feldman (1977; rat)	Fink-Heimer	•	•		●	●	●	●	•	•	•	•		
Fitzpatrick et al. (1983; monkey)	WGA-HRP												Striate cortex	
Pattern 1		•			●	●	●							Magnocellular
Pattern 2						●		●						Parvocellular
Pulvinar-lateral posterior complex														
Symonds et al. (1981; cat)	[3H]leucine	•					●	●						
Niimi and Naito (1974; cat)	Nauta-Gygax	•			●	●	●	●	•	•	•	•		
Rockland et al. (1999; monkey)	BDA	●				●	●	●	●	•	•	•		
Somatic sensory thalamus														
Ventrobasal complex (cat)														
Landry and Deschênes (1981)	HRP, intraaxonal					●	●	●	•		●	●	SI	
Penny et al. (1982)	WGA-HRP	●	●			●	●	●			•	•		
Niimi and Naito (1974)	Nauta-Gygax	•			●	●	●	●	•	•	•	•		
Other species														
Jensen and Killackey (1987; rat)	WGA-HRP in white matter			•	●	●	●	●		•	•	•	SI	
Jones (1975); Jones and Burton (1976; monkey)	[3H]proline	•	•	•	•	●	●	●	•	•	•	•		
Rausell et al. (1998; monkey)	PHA-L, fluorescent dextrans					●	●	●	•	•	•	•	SI	
Other studies														
Herkenham (1980; rat)	Tritiated amino acids													
Pattern 1		•	•			●	●	●			•			VP, MGB, LGB, Md
Pattern 2								•	●	●	●	●		Intralaminar
Pattern 3		●	●								•	•		Val, Ld, Vm, Re, P, LP, MGBm
Pattern 4		●	●		●	●	●	●	●		•	•		Val

[1]PHA-L, *Phaseolus vulgaris*-leucoagglutinin; BDA, biotinylated dextran amine; WGA-HRP, wheat germ agglutinin conjugated to horseradish peroxidase; [3H]proline, tritiated proline.

[2]●, Heavy; ●, moderate; •, light.

[3]AI, primary auditory cortex; SI; primary somatic sensory area; M, medial division of the medial geniculate body; V, lateral part of the ventral division of the medial geniculate body; Sgl, suprageniculate nucleus, lateral part; D, dorsal nucleus of the medial geniculate body; DCa, dorsal caudal division of the medial geniculate body; DD, deep dorsal nucleus of the medial geniculate body; DS, dorsal superficial nucleus of the medial geniculate body; VP,; ventral posterior auditory area; MGB, medial geniculate body; LGB, lateral geniculate body; P, posterior auditory cortex; MGBm, medial division of the medial geniculate body.

it seems appropriate to evaluate the validity of this approach. Three independent lines of evidence suggest that the profiles described here are a valid measure of thalamocortical input. First, axon-filling studies in visual cortex (Humphrey et al., 1985) and somatic sensory cortex (Landry and Deschênes, 1981) of physiologically identified afferents describe many features like those in the present study. They did not discern the class of giant axons as-

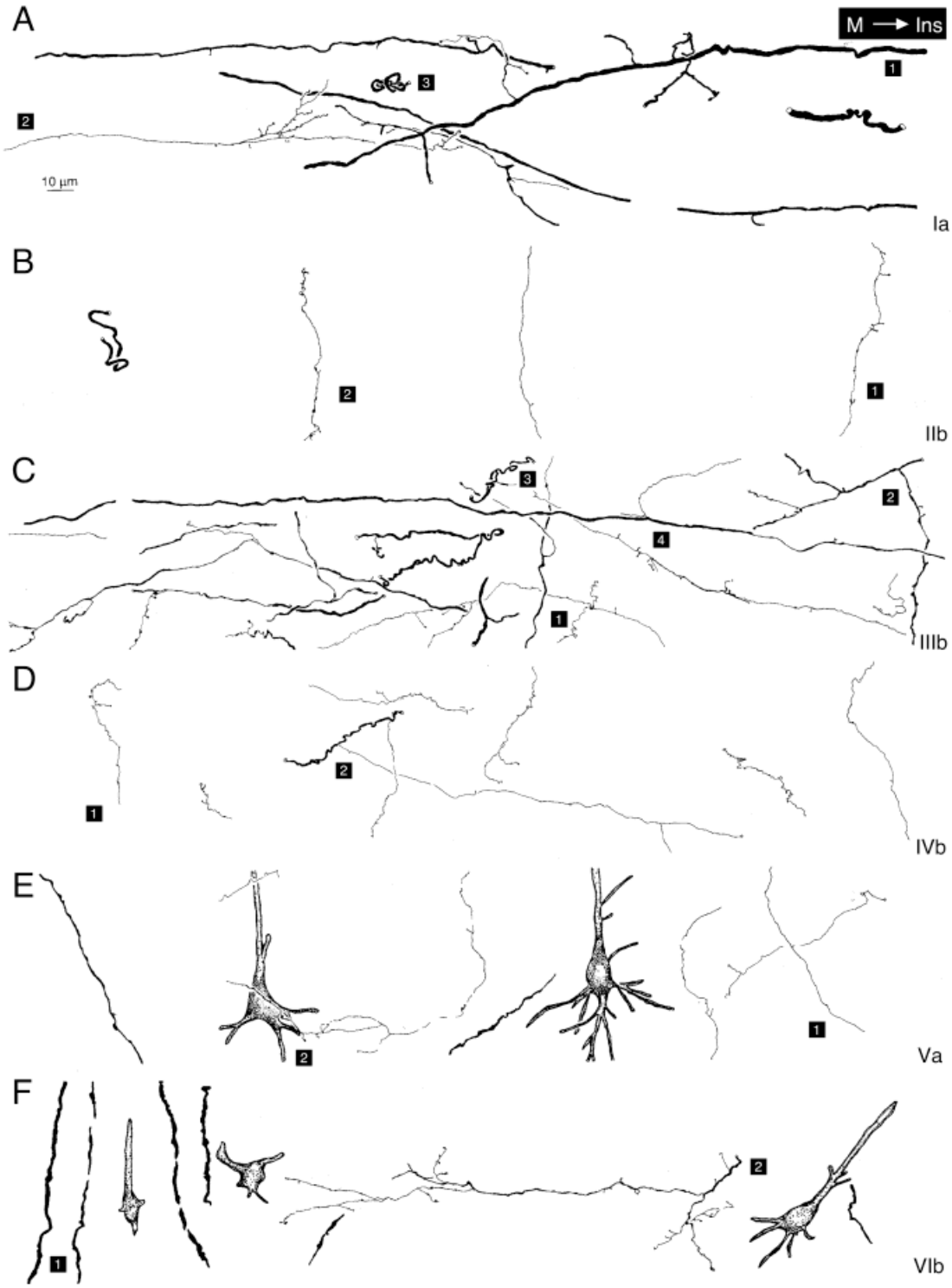

Fig. 8. Representative examples of bulk- and diffusion-filled thalamocortical axons. **A:** Layer I axons had unusually long lateral spans; some of these fibers were the thickest in our sample: (1) Coarse lateral fiber with oblique twigs at 100–200 μm intervals. (2) Finer lateral fibers formed a fan-shaped terminal plexus in layer Ia. (3) A corkscrew axon extended through much of the depth of the section, suggesting that the tangential plexus has no preferred orientation Planapochromat, N.A., 1.32, ×2,000. **B:** In layer IIb, only sparse vertical fibers were present: a fine axon with lateral twigs (1) and thin afferent with few branches (2). **C:** The lateral plexus was well developed in layer IIIb: Slender lateral axons formed delicate vertical collaterals (1); some lateral fibers had branches descending toward layer IV (2); fibers with corkscrew-like profiles were also present as in layer I (3; see A3); and the longest parent fibers gave off recurrent and remote branches along their trajectory (4). **D:** In layer IVb, the pattern resembled that in layer IIb: a fine, virtually unbranched fiber (1) and a thicker axon with an irregular trajectory and few branches (2). **E:** Slender afferent fibers predominated in layer Va, as in layers IIb (B) and IVb (D): fine axons with few branches (1) and corticogeniculate neurons (2) with little axonal labeling and extensive dendritic labeling. **F:** Some coarse vertical fibers—perhaps the parent trunks of giant layer Ia fibers—and fine lateral axons were present in layer VIb: Palisades of vertical fibers emerge from the white matter and stream across layer VI (1); and the lateral branches (2) resemble those in layer Ia (A:2) in size, shape, and disposition.

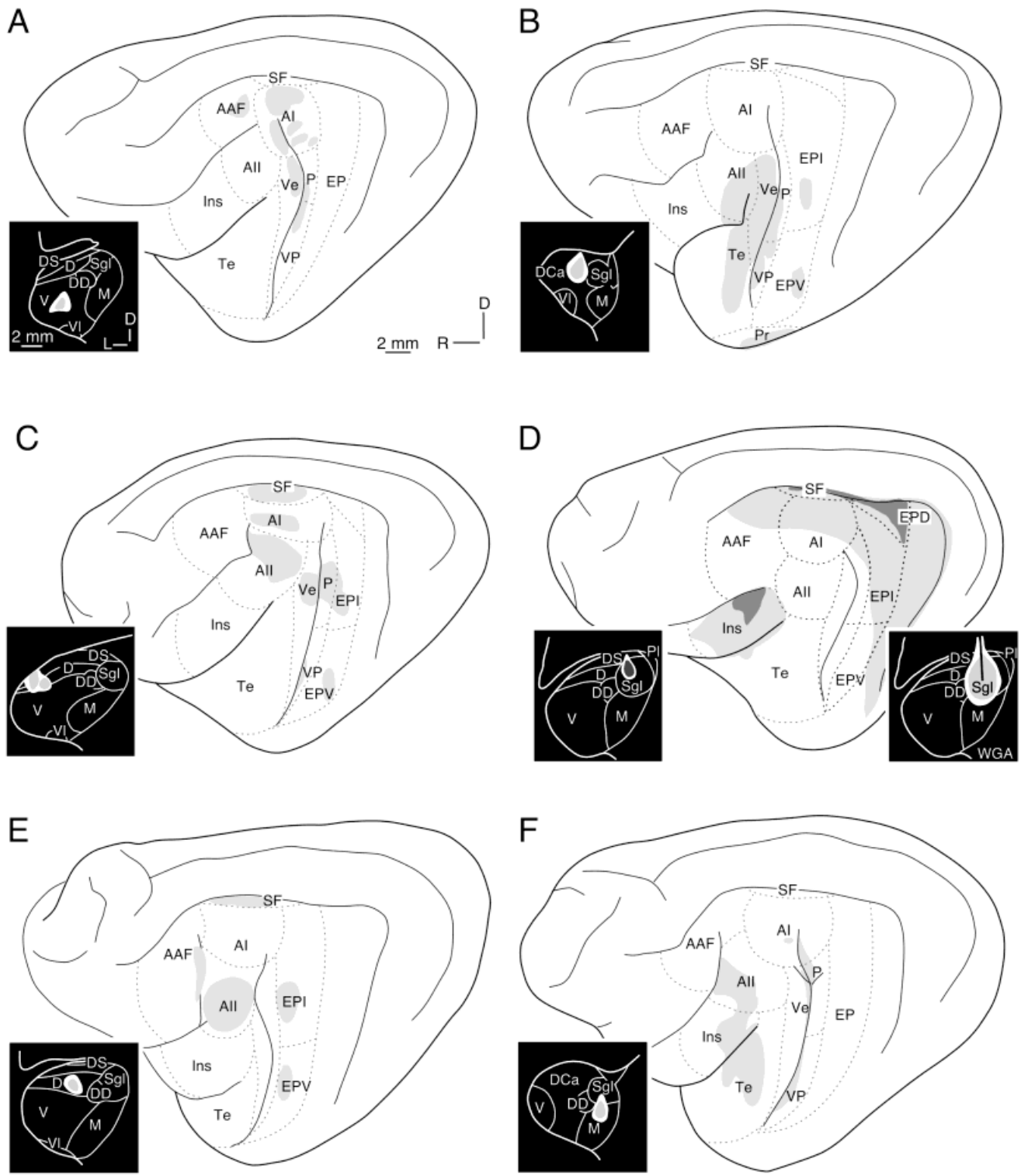

Fig. 9. Summary of additional, representative experiments. Shaded areas represent cortical targets of thalamic deposits; shading across sulci denotes labeling hidden in lateral views. Dashed lines show boundaries between fields. *Insets* (black squares) depict the injection core (white areas) and corona (stippled areas). **A:** Ventral division injections labeled primary auditory fields AI, AAF, Ve, and P. Patchy labeling was found only in AI; labeling elsewhere was continuous within an area. **B:** Caudal dorsal division (DCa) injection labeled a region from the caudal bank of the posterior ectosylvian gyrus through the rostral temporal cortex. Encroachment onto the ventral division may be responsible for the labeling in the primary fields. **C:** The lateral part of the dorsal (D) and dorsal superficial (DS) nuclei projected to AI, P, and VP and received reciprocal projections from them. The AI labeling was continuous and the deposit did not encroach deeply into the ventral division (V). **D:** Two experiments with suprageniculate (Sgl) nucleus deposits. A BDA injection <1 mm in diameter (left inset) labeled the ventral bank of the middle suprasylvian sulcus from the caudal part of the posterior ectosylvian gyrus (EPD) through the rostral part of the suprasylvian fringe (SF) area. A second experiment used 5% WGA-HRP and had a deposit ≈2 mm in diameter (right inset). In both studies, the anterograde labeling was in the posterior and middle ectosylvian gyrus (EP) and insular (Ins) cortex. The much larger WGA-HRP injections (dark stipple) confirmed the results from smaller BDA deposits. **E:** A small deposit in the medial part of the dorsal nucleus (D) labeled only nonprimary areas, whereas some primary areas (VP and AI) were labeled from the injection shown in C. **F:** A focal injection in the medial division (M) labeled many auditory fields diffusely and involved mainly AII, Ins, Te, and the posterior ectosylvian cortex (for review, see Winer, 1992).

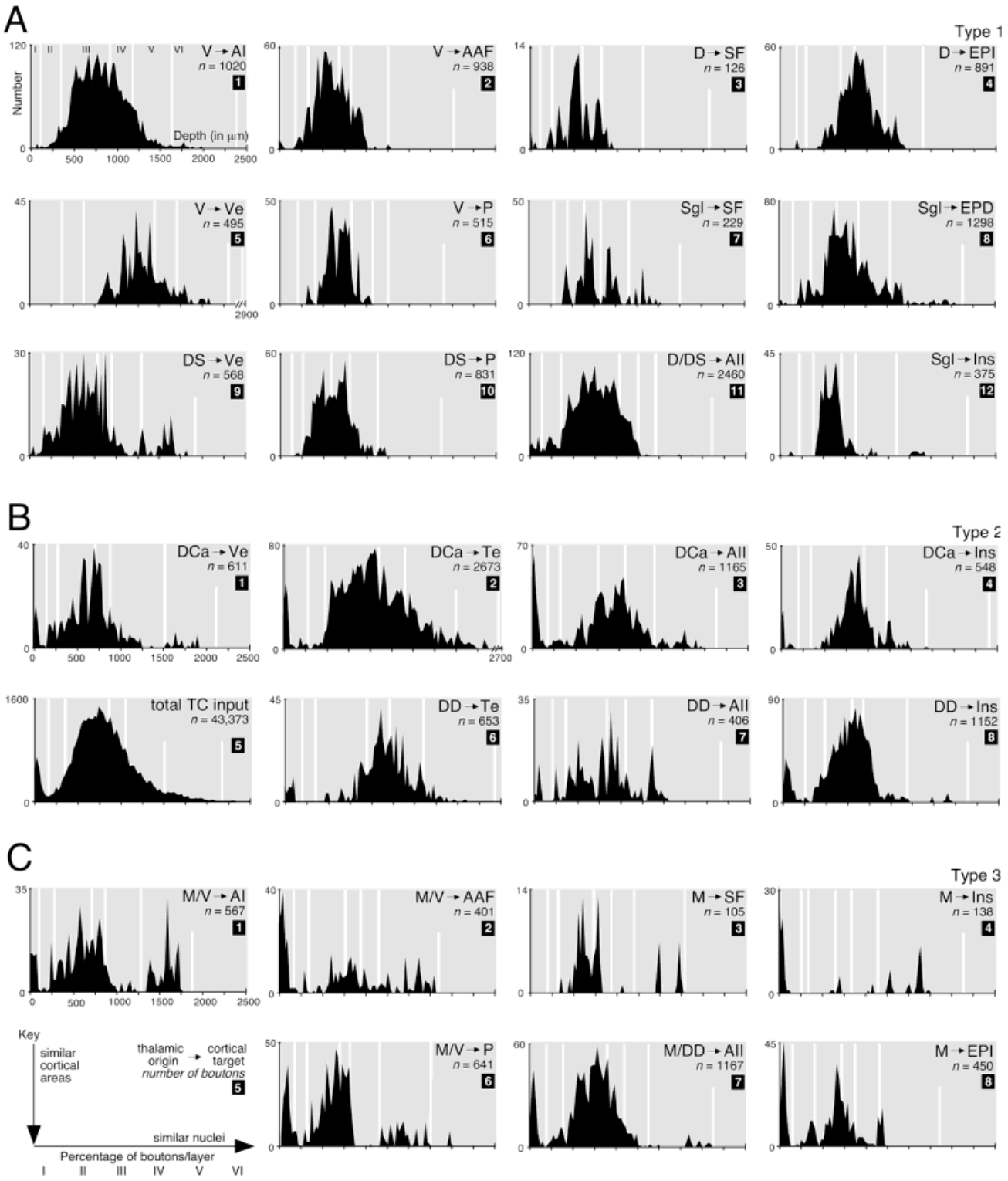

Fig. 10. Laminar distribution of the number of boutons per layer in 27 histograms from representative experiments. Ordinate, number of boutons; abscissa, cortical depth; origin and target, upper right corner; white lines, laminar borders. Common nuclear origins are grouped horizontally, whereas similar cortical areas are aligned vertically. n, total number of boutons per traverse. For details on laminar analysis, see protocol in Figure 3B. A cluster analysis (Johnson, 1992; S-PLUS) was performed to classify samples on the basis of quantitative laminar differences. A bootstrap analysis (Efron, 1993; S-PLUS) confirmed the statistical significance of these categories. **A:** The type 1 pattern had one peak concentrated in layers III–IV. **B:** The type 2 pattern had peaks in layers I and III–IV. **C:** The type 3 pattern had peaks in layer I, III–IV, VI. Graph 5 shows the average percentage of boutons per layer for types 1–3. The main difference between types 1–3 was the degree of projection to layers I and VI (see Fig. 11C:5). Type 3 had strong inputs to layer I and VI and far weaker layer III–V projections. All types had weak input to layer II.

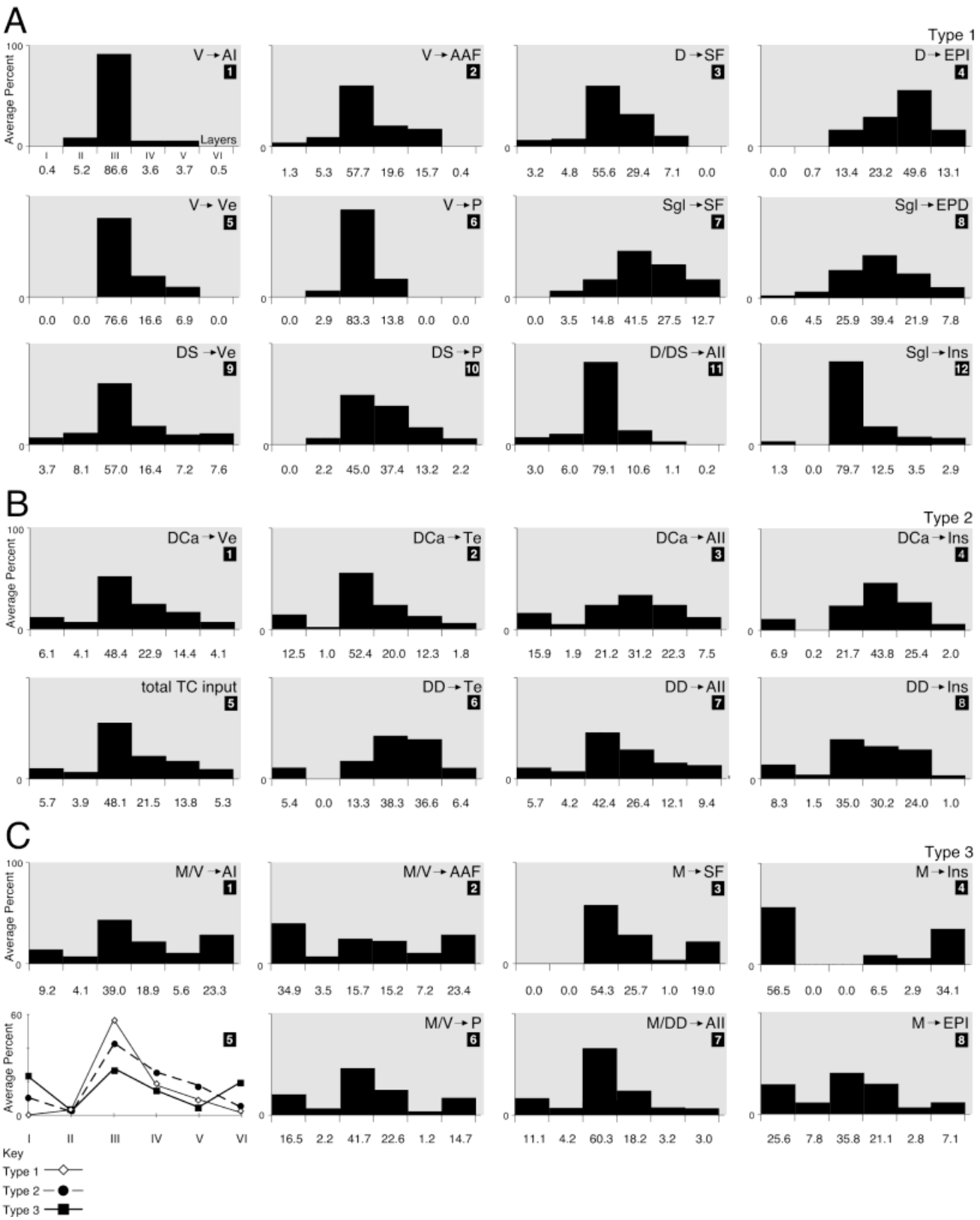

Fig. 11. Average distribution of boutons per layer in 26 histograms from the same representative experiments shown in Figure 10. Ordinate, the average percent of boutons per layer; abscissa, cortical layers and percent per layer; for protocol, see Figure 10. **A:** The type 1 pattern had one peak in layers III–IV. **B:** The type 2 pattern had two peaks, one in layer I (>5%) and the other in layers III–IV (>10%). **C:** The type 3 pattern had peaks in layer I (>9%), layers III–IV (>6% except in one experiment), and layer VI (>7%). Histogram C, #3 had no layer I labeling and strong input to layer VI. Histogram 7 in C was a medial division (M) and deep dorsal nucleus (DD) experiment (see histogram #7 in B) Histogram #5 in C shows the average percentage of boutons per layer for the three classes.

cending to layer Ia or the lateral plexus of fibers in layers III and IV. Perhaps the giant axons arise exclusively from the auditory magnocellular neuron that is unique to the medial division and is among the largest cells in the sensory thalamus (Winer and Morest, 1983a). There is no known counterpart in either the lateral geniculate body (O'Leary, 1940), pulvinar (monkey: Ogren and Hendrickson, 1979), or ventrobasal complex (Havton and Ohara, 1994). Retrograde tracing studies have demonstrated that these large neurons project to layer I when small deposits of tracer in auditory cortical sublayers are used to identify the thalamocortical neurons (Niimi et al., 1984; Mitani et al., 1987). The lateral plexus in nonprimary areas might well have been undetected in single-cell or single axon-filling experiments, because each cell might contribute just a few processes to such a projection, whereas the present deposits can reveal many such axons. Perhaps these axons are limited to nonprimary auditory cortex, especially because little is known of the details of thalamocortical projections to nonprimary areas in other modalities beyond the primary visual (Harvey, 1980) and somatic sensory (Jones and Burton, 1974) areas (Steriade et al., 1997). Supporting evidence is the presence of many of the classes of axon labeled here and those seen in Golgi preparations from young adult or mature specimens (Ramón y Cajal, 1911; Winer, 1984a,b, Winer, 1985b; Prieto and Winer, 1999). One exception is the giant fibers in layer I, which appear to represent a new substrate for thalamocortical interactions (Marín-Padilla, 1984) and may be exclusively auditory. Third, the laminar distribution of WGA-HRP (Fig. 12) or autoradiographically labeled terminals (Table 1) resembled the BDA pattern (present results), as did studies using *Phaseolus vulgaris*-leucoagglutinin (monkey: Hashikawa et al., 1995).

When the intracortical segments of intracellularly labeled corticogeniculate neurons in visual cortex were examined in the electron microscope, >85% of the structures that were identified light microscopically as boutons contained synaptic vesicles and were confirmed as presynaptic (Fariñas and DeFelipe, 1991a,b). Although the present results cannot specify synaptic implications, it is likely that the proportion of input to a specific layer will closely match the values seen here, as in quantitative autoradiographic studies (primates: Jones and Burton, 1976).

The bouton counts in the present study may have included the intracortical axonal branches of retrogradely labeled or bulk-labeled corticogeniculate neurons in layers VI and V (Figs. 3A, 5A, 7A). However, in our sample of several thousand such neurons, we have been unable to trace any of the intracortical axons back to these neurons, nor were there branches from these cells ending in the granular or supragranular layers. Perhaps neurons that are retrogradely labeled or bulk-filled are far from the injection site in the auditory thalamus and do not have their most distal branches labeled. If only the perikarya and the most distal processes accumulate labeling, then each thalamic deposit should produce a similar laminar distribution in the cortex, which is not the case (Fig. 11). Moreover, the outcome from bulk-filling studies should also differ significantly from autoradiographic studies if the former fills intracortical pyramidal cell collaterals, whereas the latter does not. Because the results are similar with the two methods, perhaps these fibers do not contribute significantly to our results.

Functional implications for laminar processing

Because the thalamocortical projections in this study showed considerable laminar divergence—averaging ≈5 layers (Fig. 11)—it seems appropriate to consider how this might influence cortical and thalamic function. In some cases, such as layer II, this is more difficult, because too little of its functional role is known (Winer, 1985b); in others, like layer IV (Winer, 1984a), it is easier to propose functional hypotheses. The following remarks pertain chiefly to AI, where most of the physiological and anatomical studies have been made.

Layer I. In most samples (32 of 41; 78%), layer I received a projection, ranging from 0.4% of the total projection across layers (Fig. 11A, 1) to 56.5% (Fig. 11C, 4). Four of the six samples without such a projection were in experiments with a type 1 pattern (Fig. 11A), where >50% of the labeling was in layers III–IV (except in one instance: Fig. 11A, 4).

There are two noteworthy facets of the projection to layer I. First, it is almost entirely in layer Ia, the sole exceptions being experiments with heavy input (Fig. 10B, 2) or a very small projection to layer I (Fig. 10A, 11). Prominent in layer Ia neuropil are the distal dendrites of layer II pyramidal cells (Winer, 1985b) and apical dendrites from some pyramids in layers III (Winer, 1984c), V (Sousa-Pinto, 1973b), and VI (Prieto and Winer, 1999). Intrinsic components include the lateral dendrites of horizontal and multipolar cells, both of which are GABAergic (Winer and Larue, 1989). There are many fine, GABAergic puncta in layer Ia. Perhaps in many species there is confluent (Fleischhauer and Laube, 1977) medial division glutamatergic (rat: Popowits et al., 1988) input to thalamic neurons (rat: Ryugo and Killackey, 1974) and projections from local GABAergic neurons to the distal dendrites of presumptive commissural or corticofugal neurons (Sousa-Pinto et al., 1975; rat: Winer and Larue, 1989). This pathway could modulate higher order processes, such as the transition from sleeping to waking (Cauller, 1995), or help detect novel stimuli hidden in noise. These roles are also consistent with physiological hypotheses about medial division function (Winer and Morest, 1983a), such as a role in fear conditioning (rat: LeDoux et al., 1986) or physiological plasticity (Gerren and Weinberger, 1983). Some of these functions may require cortical participation, because decorticate preparations show deficits (Steriade, 1997).

A second observation augments this hypothesis. The giant fibers ascending to layer I, to our knowledge, are the largest thalamocortical axons known (Jones, 1985; Ste-

Fig. 12. Auditory thalamocortical projection patterns from WGA-HRP experiments. A,C,E: Darkfield areal views of labeling. Planachromat, N.A. 0.10, ×50). B,D,F: High-power views. Dots indicate the locus of B, D, and F. **A:** Ventral division projection to AI. White arrows, foci of labeling. Input is concentrated in layers III–IV. The corticothalamic layer VI projection is robust. **B:** Input is continuous in layers III–V. **C:** Caudal dorsal division projection to temporal cortex (Te), with heaviest labeling in layers I and III–IV. **D:** Dense input targets layers IIIb–IV. **E:** Medial division input to insular cortex (Ins) labeled layers I, III–IV, and VI. **F:** Projections to layers Ia and IV predominated, although these were much sparser than those in areas AI or Te after deposits similar in volume.

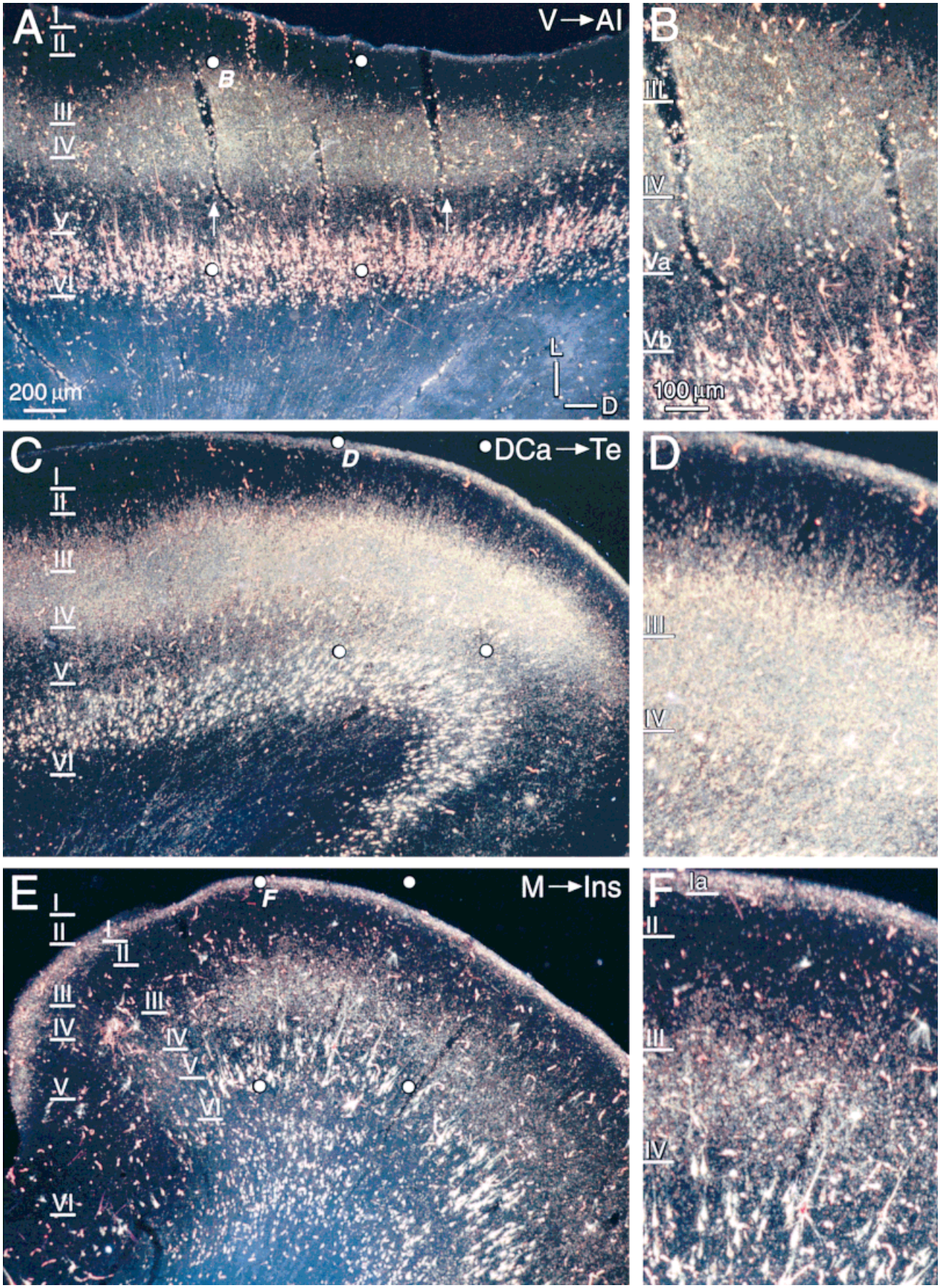
A
V→AI
B
I
II
III
IV
V
VI
200 µm
L
D
B
III
IV
Va
Vb
100 µm
C
D
•DCa→Te
I
II
III
IV
V
VI
D
III
IV
E
F
M→Ins
I
II
III
IV
V
VI
F
Ia
II
III
IV

Figure 12

riade et al., 1997). They have not been reported elsewhere, perhaps because their size suggests they might be dendritic (rat: Winer and Larue, 1988) or their relative rarity could impede their detection in Golgi preparations. Even if their overall contribution is minute numerically, their signals should reach layer Ia before those of the far finer afferents to layer IV. Because the former projection is a cardinal feature of the medial division, involving all 14 areas identified here as auditory cortex (Table 4), it could synchronize remote activity across or provide a common input to functionally disparate areas. Such projections would seem to be essential to coordinate auditory coding for global spatial localization (Bregman, 1990; Middlebrooks et al., 1994) with the appropriate limbic input for autonomic and cognitive adjustments to the biological significance of sound (Davis et al., 1997).

Layer II. In most cases (26 of 41; 63%), layer II received thalamic input (Fig. 10), although it had the smallest average projection (2%; Fig. 11B, 5). Because little is known of layer II physiology, we can offer a few suggestions in accord with its anatomical properties (Winer, 1985b; Prieto et al., 1994a,b). In layer I, we emphasized lateral interactions between thalamocortical axons (Fig. 8A) and the distal dendrites of corticofugal cells. In layer II, in contrast, most afferent and intrinsic axons are arranged vertically (Figs. 3A, II; 5A, II; 7A, II; 8, IIb). This organization is consistent with the conspicuous dendritic bundles in the granular layers and a feature common to much of auditory cortex (Fig. 1C,E; Sousa-Pinto, 1973b). A possible role for thalamic input to neurons that usually are regarded as intrinsic (Winer, 1985b) is that of adjusting receptive fields subsequent to higher order processing, as similar arrangements in the visual system can shunt or enhance transmission through the supragranular layers (Gilbert, 1977). A second possible influence of such projections is to endow otherwise classical receptive fields with an extended range of responses to complex stimuli, again like visual cortex neurons (Allman et al., 1985). Rodent AI can reorganize its physiological representation of frequency in response to experience, suggesting that intrinsic circuitry plays a role (rat: Kilgard and Merzenich, 1998) as well as subcortical centers (rat: Lane et al., 1995). These changes could require cholinergic-glutamatergic interactions to mediate synaptic efficacy (rat: Metherate and Ashe, 1995).

Layer III. Almost half of the boutons in a typical experiment (48%; Fig. 11B, 5) were in layer III, only 1 of 41 samples (2.4%) had none (Fig. 11C, 4), and 25 of 26 had a larger concentration in layer IIIb than in layer IIIa (Fig. 10A, 9). This sublaminar difference suggests that commissural cells of origin, which are concentrated in layer IIIa (Code and Winer, 1985) may receive sharply tuned thalamic afferents to their basal dendrites and fibers from more widely tuned thalamic neurons on their apical processes in layers II and I (monkey: Hendry and Jones, 1983). Layer IIIb also contains a rich plexus of horizontal axons (Fig. 8, 3b) second in size only to those in layer I (Fig. 8, Ia).

The results suggest a degree of sublaminar independence between the thalamocortical and commissural systems. Vertical or columnar modules would be well suited, at least in primary areas (Fleischhauer, 1974), to the spatiotemporal segregation of afferent signals to a specific frequency (Merzenich et al., 1975), a particular point in the visual field (Tusa et al., 1978), or a site on the skin

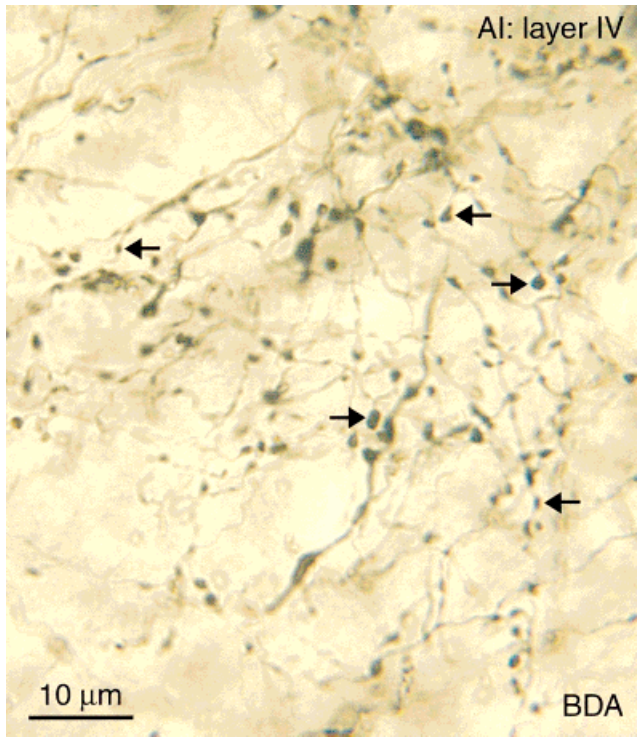

Fig. 13. Representative terminal-rich plexus of BDA-labeled axons in layer IV of AI. Swellings (arrowheads) are interspersed periodically along fine axonal tendrils in a lacy texture. The swellings were classified as boutons and used for the analyses in Figures 3, 5, 7, 10, 11. Boutons in AI ranged from 0.5 μm to 2.0 μm in diameter. Planapochromat, N.A. 1.32, ×1,250.

(Felleman et al., 1983). This agrees with the observation that, without concomitant ascending sensory stimulation and the actions of cholinergic nucleus basalis neurons (rat: Kilgard and Merzenich, 1998), there is little associative retuning in AI (Weinberger and Diamond, 1987). In nonprimary areas, such as AII, such retuning is evoked far more readily (Diamond and Weinberger, 1984). Whether such retuning depends on purely intrinsic cortical mechanisms or reflects plasticity in associated thalamic or brainstem nuclei (see above) is an open question. Perhaps the robust lateral plexus in nonprimary auditory cortex has a role in such plasticity. The tangential breadth and spatial overlap of fibers with different tuning properties could be related to the broad frequency tuning curves in nonprimary cortex (Schreiner and Cynader, 1984).

Layer IV. Whereas the mean percentage of input to layer IV in all experiments (Fig. 11B, 9) was less than half of that to layer III (21.5% and 48.1%, respectively), layer IV was labeled significantly in every sample. Layer IV, along with layer I, has the largest proportion of GABAergic neurons in AI, ≈26% (Prieto et al., 1994a), and its neurons are mainly nonpyramidal cells (Winer, 1984a) with predominantly local projections (Winguth and Winer, 1986). It is neither a source for, nor a target of, commissural projections (Code and Winer, 1985, 1986).

The consistency of input to layer IV reflects contributions from each of the three main parts of the medial geniculate body. Elsewhere, we have designated these as

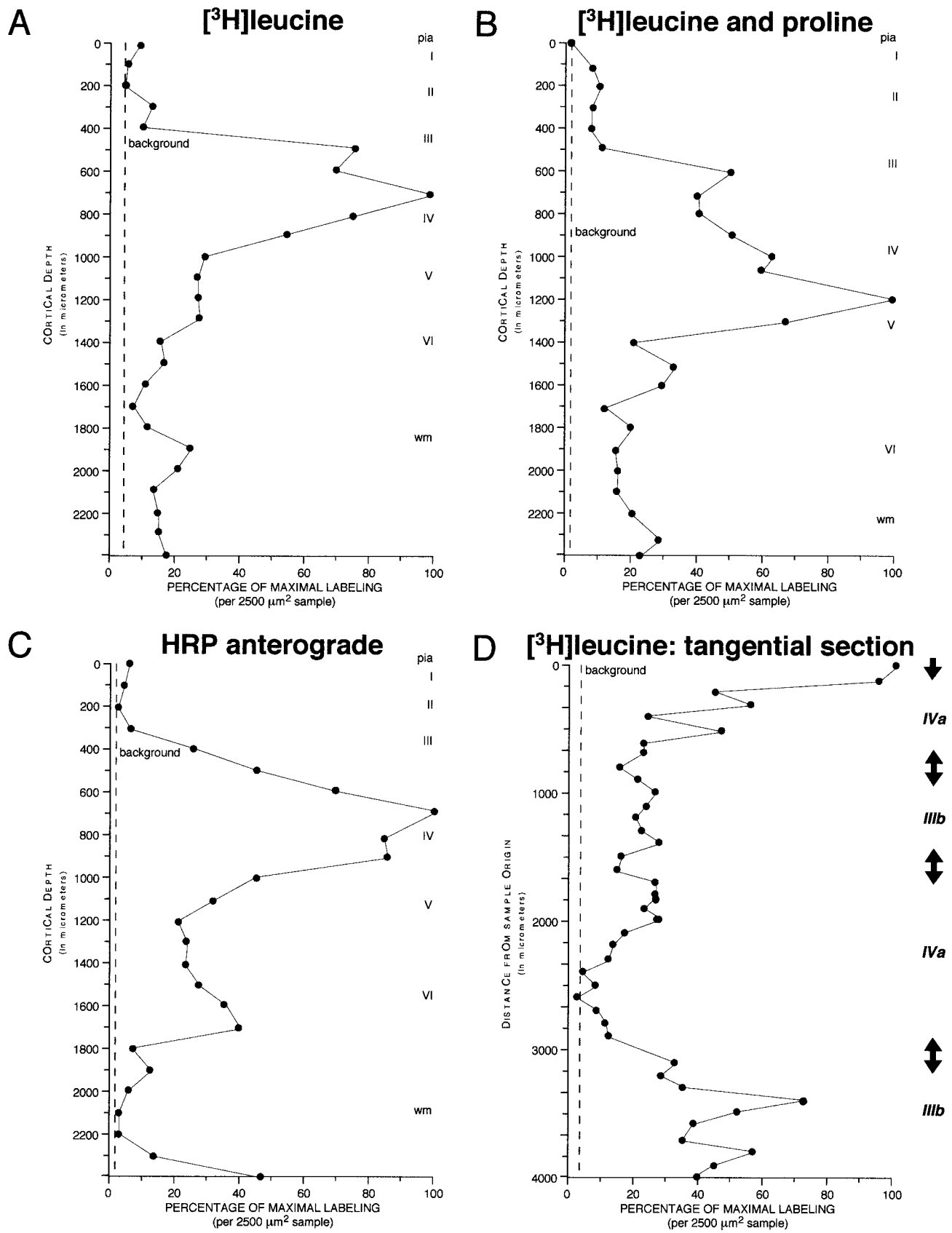

Fig. 14. Comparisons of autoradiographic grain counts and HRP granular labeling in AI after ventral division deposits. **A:** Studies using tritiated leucine ([^{3}H]leucine) had grain counts well above background (dashed line) and peaks in layer IIIb, with most silver grains in layers III and IV. **B:** Experiments with [^{3}H]leucine and proline had single peaks in layers III and IV. **C:** Deposits of WGA-HRP produced anterograde input like that shown in A and B, with a peak in layer IIIb–IVa. This ventral division projection to AI pattern resembled the projection seen with BDA (Figs. 10, 11). **D:** The distribution of [^{3}H]leucine labeling in a flat-mounted hemisphere sectioned tangentially showed a periodic distribution within AI (compare with Fig. 3C).

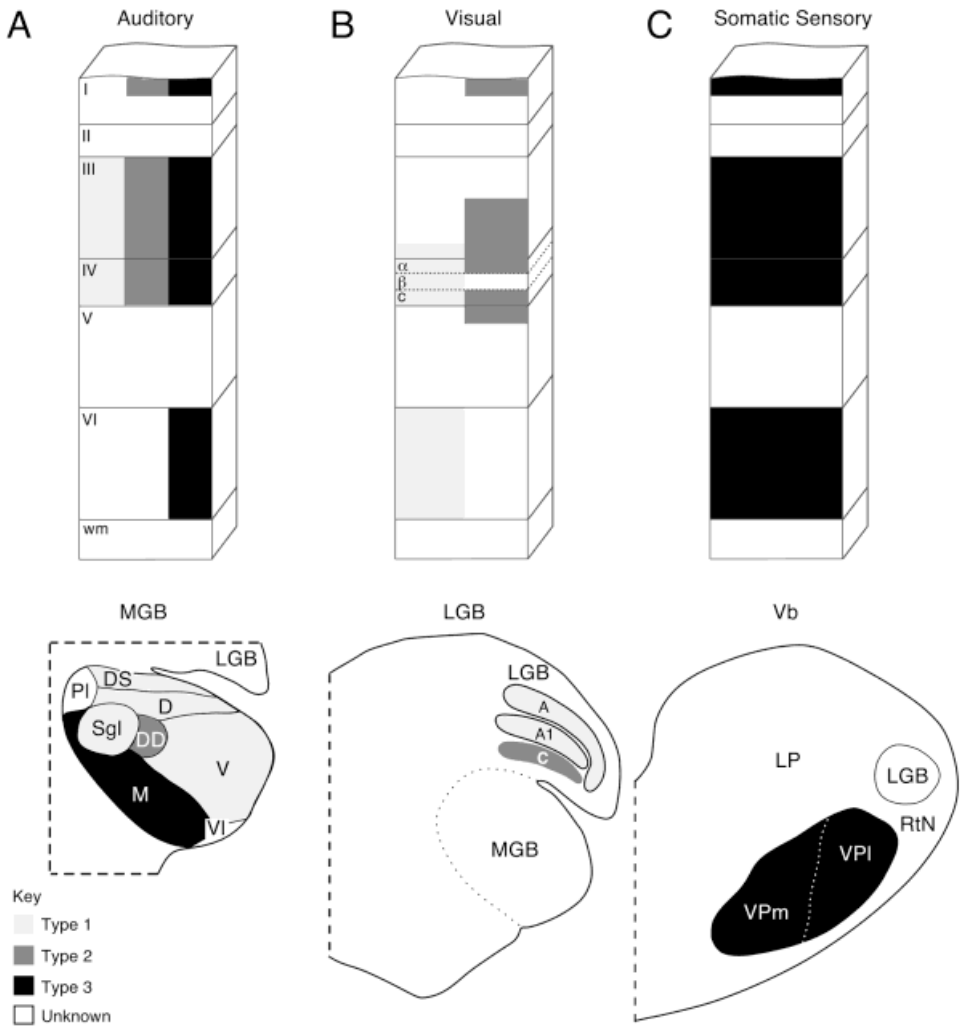

Fig. 15. Summary of thalamic laminar input to sensory cortex. The patterns in visual and somatic sensory cortex are compared to the three auditory thalamic laminar distribution patterns. Type 1 does not involve layers I and VI, whereas type 3 does. **A:** Auditory thalamocortical input had three patterns: the ventral division (V) and the dorsal (D), dorsal superficial (DS), and suprageniculate (Sgl) nuclei had a type 1 pattern; the deep dorsal (DD) and caudal dorsal (DCa; not shown) nuclei had a type 2 arrangement; and the medial division (M) had a type 3 distribution. **B:** Visual thalamocortical inputs from the lateral geniculate body A, A1, and C laminae resemble type 1 and 2 auditory thalamic patterns. Laminae A and A1 project to layers IV and VI; lamina C terminates in layers I, III, and IV. **C:** Somatic sensory thalamic axons end layers I, III, IV, and VI, much like the type 3 auditory projection pattern.

the purely auditory (lemniscal) ventral division, the multisensory medial division (extralemniscal), and the dorsal division (lemniscal adjunct), whose functional status is obscure (Winer and Morest, 1983a). Perhaps some laminar patterns are conserved in primary and nonprimary cortex, and each medial geniculate body division has lamina-specific relations with its cortical targets, even if these layers differ from area to area (Winer, 1992). Laminar parallels, as noted above, do not necessarily entail functional parallels. Thus, whereas lemniscal (Fig. 10A, 1) and lemniscal adjunct (Fig. 10B, 2) nuclei each terminate heavily in layer IV, the former has a clustered and topographic pattern of input (Fig. 2D–F), whereas the latter has no discernible areal topography (Fig. 4D–F). Perhaps the functional role of layer IV is area-specific, a hypothesis consistent with some (Merzenich et al., 1975; Schreiner and Cynader, 1984) but not all (Eggermont, 1998) of the physiological data available. It remains to compare neuronal response profiles in layer IV in different areas.

Layer V. An unexpected finding was the density of input to layer V, averaging 13.8% of the total and present in 25 of 26 samples (Fig. 11). Layer V has diverse connections in AI, with significant projections to the thalamus mainly from the lower half and input to the commissural and corticocollicular systems from the upper half (Kelly and Wong, 1981; rat: Games and Winer, 1988). The thalamic projection in the present experiments was concentrated in the superficial half, except in an experiment with the lowest projection density in our entire sample (Fig. 10C, 3). If the same sublaminar projection patterns in AI prevail in other areas, then layer V commissural and corticocortical neurons may preferentially receive thalamic input at the expense of corticocollicular and corticothalamic cells. It also suggests that, despite the global

thalamocortical/corticothalamic reciprocity (rat: Winer and Larue, 1987) or parity (Deschênes et al., 1998), this principle, at least in this system, does not extend to link nuclei to layers but only to link nuclei to areas.

Layer VI. Layer VI has the most diverse set of connections in AI (Prieto and Winer, 1999) and a significantly lower proportion of GABAergic neurons (Prieto et al., 1994a) and puncta (Prieto et al., 1994b) than other layers. It received among the lowest proportion of thalamic input (Fig. 11B, 5), as might be expected, although terminals were found in 21 of 26 instances. Projections to layers I, II, and VI (Fig. 11B, 5) constitute <15% of the total, whereas the input to layers III–V was >85%. Thus, although all layers participate in thalamocortical processing, there is a watershed between layers I, II, and VI and layers III–V. This suggests that, whereas thalamic influence can reach to every cortical layer in one form or another, the global laminar pattern of input is principally to the granular and supragranular layers (including layer V) and secondarily to infragranular targets. The presumably weaker, GABAergic influences on layer VI cells suggest that neurons postsynaptic to them receive information that has been processed differently than that in layers III–IV, a hypothesis that remains to be tested.

We have proposed (Prieto and Winer, 1999) that the diversity of neurons and connections in layer VI is an ontogenetic (and perhaps a phylogenetic) reflection of the fundamental role of this layer in neural development, a role that, not coincidentally in our view, links it with layer I cytologically (Prieto et al., 1994b; Prieto and Winer, 1999) and hodologically (opossum and hedgehog: Killackey and Ebner, 1972; rat: Ryugo and Killackey, 1974). Insofar as layer VI represents a protocortical entity that is essential for the construction of other layers, perhaps it contains more types of neurons and a wider constellation of connections than they do; both of these predictions have been verified (Prieto and Winer, 1999). What the functional implication of a small thalamic input to layer VI may be is unknown. Perhaps every layer must receive some thalamic input simply to coordinate activity temporally within and across functionally discrete columns. Alternatively, this input could evoke or provide a basis for the establishment of reciprocal corticogeniculate linkages (rat: Winer and Larue, 1987) that themselves elicit signals in thalamic neurons, enabling their growth toward specific layers (rat: Henke-Fahle et al., 1996) and beginning the extended process of laminar (ferret: Finney et al., 1998) and areal (rat: Wall, 1988) functional differentiation. Conversely, these connections may simply be the developmental residue of a period when the thalamic relations to the neocortex were limited largely to the infragranular layers.

Implications for cortical processing

The three laminar patterns of thalamocortical input have different implications for the cortical redistribution of thalamic information. For example, the powerful input to layers III–IV (type 1; Fig. 15A) in the primary fields (AI, AAF, P, and VP) suggests that cells in layers I and II that are concerned largely with intrinsic projections (Winguth and Winer, 1986) receive a different form of thalamic input. Layer V and VI neurons, which are mainly corticofugal (Kelly and Wong, 1981), receive less thalamic influence in the type 1 pattern. In contrast, the type 2 pattern includes many nonprimary/parabelt areas (AII, Ins, and Te) and has a far wider laminar distribution than the type 1 pattern. The type 3 projection is still more variable, and it may extend chiefly to layers with intrinsic and corticofugal projections as well as thalamic-recipient laminae. Perhaps these patterns underlie functional attributes. Thus, volleys of ascending input to layers I–II and layers V–VI may be delayed temporally in the type 1 pattern but not in the type 3 pattern. The type 2 pattern suggests that layer V corticofugal cells in nonprimary areas are more strongly affected by the thalamus than the corresponding cells in AI. The type 1 pattern should affect layer V much more strongly (Fig. 11A; 11 of 12 examples) than layer VI (Fig. 11A; 5 of 12 examples). Perhaps some corticogeniculate neurons operate more independently of thalamic input than corticocollicular cells.

These laminar and areal differences may be significant for intercortical hierarchical patterns of connection (Rouiller et al., 1991) and for areal functional specializations (Eggermont, 1998; Heil and Irvine, 1998). Subtle physiological differences among primary fields (Schreiner and Urbas, 1988) may reflect distinct thalamocortical areal arrangements.

Developmental perspective

The mature patterns of thalamic input are the result of a long ontogenetic process of cellular proliferation, migration, differentiation, the establishment of laminar identity, and the elaboration of cortical connectivity. Some of the earliest events in thalamic ingrowth to the neocortex suggest that input concentrates in the centralmost layers (rat: Molnár and Blakemore, 1991), which will probably constitute layers III and IV in the adult (rat: Miller, 1981). This primordial pattern occurs even when immature thalamic nuclei or presumptive cortical areas are cultured together in combinations that would not occur normally (Molnár and Blakemore, 1991). Perhaps the type 1 pattern is older in phylogeny, and the primary sensory areas represent the essential ancestral condition from which the (presumably more variable and complex) type 2 and type 3 patterns later emerged (platypus and echidna: Krubitzer et al., 1995). In mammals with a less differentiated cortical organization—such as marsupials (Lende, 1963) and insectivores (Lende and Sadler, 1967; Batzri-Izraeli et al., 1990)—thalamic input may have a more specific laminar distribution than it does in the cat (present results) and monkey (Hashikawa et al., 1995).

CONCLUSIONS

The present results suggest that there are substantial differences among thalamic nuclei in one modality with regard to their laminar terminations and the structure of the thalamocortical axons. For example, each of the nuclei studied projected to many areas and had significant terminations in several layers. Moreover, the subdivisions differ with regard to their axonal morphology and patterns of termination, with the largest axons arising from the medial division and targeting layer I, whereas the ventral division alone has a periodic clustered terminal arrangement that consists almost entirely of medium-sized axons. These differences imply that the actions of the thalamus on the cortex may differ on both nuclear grounds and areal grounds and in ways that await exploration.

ACKNOWLEDGMENTS

Mr. Jaimyoung Kwon kindly provided helpful statistical advice and consultation. Our colleagues, Drs. Steven W. Cheung, Heather L. Read, Christoph E. Schreiner, and Mr. Lee Miller, Ph.C., from the W.M. Keck Center for Neuroscience at the University of California School of Medicine at San Francisco, commented constructively on an early draft. Mr. David T. Larue offered useful suggestions as well. We thank Dr. Barbara A. Peterson for sharing her experimental results.

LITERATURE CITED

Adams JC. 1981. Heavy metal intensification of DAB-based HRP reaction product. J Histochem Cytochem 29:775.

Aitkin LM. 1973. Medial geniculate body of the cat: responses to tonal stimuli of neurons in medial division. J Neurophysiol 36:275–283.

Aitkin LM. 1976. Tonotopic organization at higher levels of the auditory pathway. In: Porter R, editor. Int Rev Physiol, Neurophysiol II. Baltimore: University Park Press. p 249–279.

Aitkin L. 1990. The auditory cortex: structural and functional bases of auditory perception. London: Chapman & Hall.

Aitkin LM, Prain SM. 1974. Medial geniculate body: unit responses in the awake cat. J Neurophysiol 37:512–521.

Aitkin LM, Webster WR. 1972. Medial geniculate body of the cat: organization and responses to tonal stimuli of neurons in ventral division. J Neurophysiol 35:365–380.

Aitkin LM, Calford MB, Kenyon CE, Webster WR. 1981. Some facets of the organization of the principal division of the cat medial geniculate body. In: Syka J, Aitkin LM, editors. Neuronal mechanisms of hearing. London: Plenum Publishing Company. p 163–181.

Allman J, Miezin F, McGuiness E. 1985. Stimulus specific responses from beyond the classical receptive field: neurophysiological mechanisms for local-global comparisons in visual neurons. Annu Rev Neurosci 8:407–430.

Andersen RA, Knight PL, Merzenich MM. 1980a. The thalamocortical and corticothalamic connections of AI, AII, and the anterior auditory field (AAF) in the cat: evidence for two largely segregated systems of connections. J Comp Neurol 194:663–701.

Andersen RA, Roth GL, Aitkin LM, Merzenich MM. 1980b. The efferent projections of the central nucleus of the inferior colliculus in the cat. J Comp Neurol 194:649–662.

Aumann TD, Ivanusic J, Horne MK. 1998. Arborisation and termination of single motor thalamocortical axons in the rat. J Comp Neurol 396:121–130.

Batzri-Izraeli R, Kelly JB, Glendenning KK, Masterton RB, Wollberg Z. 1990. Auditory cortex of the long-eared hedgehog (*Hemiechinus auritus*) I. Boundaries and frequency representation. Brain Behav Evol 36:237–248.

Berman AL. 1968. The brain stem of the cat: a cytoarchitectonic atlas with stereotaxic coordinates. Madison, WI: University of Wisconsin Press.

Blasdel GG, Lund JS. 1983. Termination of afferent axons in macaque striate cortex. J Neurosci 3:1389–1413.

Bowman EM, Olson CR. 1988a. Visual and auditory association areas of the cat's posterior ectosylvian gyrus: cortical afferents. J Comp Neurol 272:30–42.

Bowman EM, Olson CR. 1988b. Visual and auditory association areas of the cat's posterior ectosylvian gyrus: thalamic afferents. J Comp Neurol 272:15–29.

Brandner S, Redies H. 1990. The projection of the medial geniculate body to field AI: organization in the isofrequency dimension. J Neurosci 10:50–61.

Brandt HM, Apkarian AV. 1992. Biotin-dextran: a sensitive anterograde tracer for neuroanatomic studies in rat and monkey. J Neurosci Methods 45:35–40.

Bregman AS. 1990. Auditory scene analysis. The perceptual organization of sound. Cambridge, MA: MIT Press.

Calford MB. 1983. The parcellation of the medial geniculate body of the cat defined by the auditory response properties of single units. J Neurosci 3:2350–2364.

Calford MB, Aitkin LM. 1983. Ascending projections to the medial geniculate body of the cat: evidence for multiple, parallel auditory pathways through the thalamus. J Neurosci 3:2365–2380.

Cauller L. 1995. Layer I of primary sensory neocortex: where top-down converges upon bottom-up. Behav Brain Res 71:163–170.

Cetas JS, de Venecia RK, McMullen NT. 1999. Thalamocortical afferents of Lorente de Nó: medial geniculate axons that project to primary auditory cortex have collateral branches to layer I. Brain Res 830:203–208.

Cipolloni PB, Keller A. 1989. Thalamocortical synapses with identified neurons in monkey primary auditory cortex: a combined Golgi/EM and GABA/peptide immunocytochemistry study. Brain Res 492:347–355.

Clarey JC, Barone P, Imig TJ. 1992. Physiology of thalamus and cortex. In: Popper AN, Fay RR, editors. Springer handbook of auditory research, vol. 2: the mammalian auditory pathway: neurophysiology. New York: Springer-Verlag, p 232–334.

Clascá F, Llamas A, Reinoso-Suárez F. 1997. Insular cortex and neighboring fields in the cat: a redefinition based on cortical microarchitecture and connections with the thalamus. J Comp Neurol 384:456–482.

Code RA, Winer JA. 1985. Commissural neurons in layer III of cat primary auditory cortex (AI): pyramidal and non-pyramidal cell input. J Comp Neurol 242:485–510.

Code RA, Winer JA. 1986. Columnar organization and reciprocity of commissural connections in cat primary auditory cortex (AI). Hear Res 23:205–222.

Colwell S. 1975. Thalamocortical-corticothalamic reciprocity: a combined anterograde-retrograde tracer technique. Brain Res 92:443–449.

Cowan WM, Gottlieb DI, Hendrickson AE, Price JL, Woolsey TA. 1972. The autoradiographic demonstration of axonal connections in the central nervous system. Brain Res 37:21–51.

Davis M, Walker DL, Lee Y. 1997. Amygdala and bed nucleus of the stria terminalis: differential roles in fear and anxiety measured with the acoustic startle reflex. Phil Trans R Soc (Lond) B 352:1675–1687.

de Venecia RK, McMullen NT. 1994. Single thalamocortical axons diverge to multiple patches in neonatal auditory cortex. Brain Res Dev Brain Res 81:135–142.

Deschênes M, Veinante P, Zhang Z-W. 1998. The organization of corticothalamic projections: reciprocity versus parity. Brain Res Brain Res Rev 28:286–308.

Diamond DM, Weinberger NM. 1984. Physiological plasticity of single neurons in auditory cortex of the cat during acquisition of the pupillary conditioned response: II. Secondary field (AII). Behav Neurosci 98:189–210.

Diamond IT, Jones EG, Powell TPS. 1969. The projection of the auditory cortex upon the diencephalon and brain stem of the cat. Brain Res 15:305–340.

Efron B. 1993. An introduction to the bootstrap. New York: Chapman and Hall.

Eggermont JJ. 1998. Representation of spectral and temporal sound features in three cortical fields of the cat. Similarities outweigh differences. J Neurophysiol 80:2743–2764.

Fariñas I, DeFelipe J. 1991a. Patterns of synaptic input on corticocortical and corticothalamic cells in the cat visual cortex. I. The cell body. J Comp Neurol 304:53–69.

Fariñas I, DeFelipe J. 1991b. Patterns of synaptic input on corticocortical and corticothalamic cells in the cat visual cortex. II. The axon initial segment. J Comp Neurol 304:70–77.

Felleman DJ, Wall JT, Cusick CG, Kaas JH. 1983. The representation of the body surface in S-I of cats. J Neurosci 3:1648–1669.

Ferster D, LeVay S. 1978. The axonal arborizations of lateral geniculate neurons in the striate cortex of the cat. J Comp Neurol 182:923–944.

Finney EM, Stone JR, Shatz CJ. 1998. Major glutamatergic projection from subplate into visual cortex during development. J Comp Neurol 398: 105–118.

Fitzpatrick D, Itoh K, Diamond IT. 1983. The laminar organization of the lateral geniculate body and the striate cortex in the squirrel monkey (*Saimiri sciureus*). J Neurosci 3:673–702.

Fleischhauer K. 1974. On different patterns of dendritic bundling in the cerebral cortex of the cat. Zeit Anat Entwicklungsgesch 143:115–126.

Fleischhauer K, Laube A. 1977. A pattern formed by preferential orientation of tangential fibres in layer I of rabbit's cerebral cortex. Anat Embryol 151:233–240.

Friedlander MJ, Lin C-S, Stanford LR, Sherman SM. 1980. Morphology of functionally identified neurons in lateral geniculate nucleus of the cat. J Neurophysiol 46:80–129.

Games KD, Winer JA. 1988. Layer V in rat auditory cortex: projections to the inferior colliculus and contralateral cortex. Hear Res 34:1–26.

Gerren RA, Weinberger NM. 1983. Long term potentiation in the magnocellular medial geniculate nucleus of the anesthetized cat. Brain Res 265:138–142.

Gilbert CD. 1977. Laminar differences in receptive field properties of cells in cat primary visual cortex. J Physiol (Lond) 268:391–421.

Guillery RW. 1966. A study of Golgi preparations from the dorsal lateral geniculate nucleus of the adult cat. J Comp Neurol 128:21–50.

Hackett TA, Stepniewska I, Kaas JH. 1998. Thalamocortical connections of the parabelt auditory cortex in macaque monkeys. J Comp Neurol 400:271–286.

Harvey AR. 1980. The afferent connexions and laminar distribution of cells in area 18 of the cat. J Physiol (Lond) 302:483–505.

Hashikawa T, Molinari M, Rausell E, Jones EG. 1995. Patchy and laminar terminations of medial geniculate axons in monkey auditory cortex. J Comp Neurol 362:195–208.

Havton LA, Ohara PT. 1994. Cell body and dendritic tree size of intracellularly labeled thalamocortical projection neurons in the ventrobasal complex of cat. Brain Res 651:76–84.

He J, Hashikawa T. 1998. Connections of the dorsal zone of cat auditory cortex. J Comp Neurol 400:334–348.

Heil P, Irvine DRF. 1998. Functional specialization in auditory cortex: responses to frequency-modulated stimuli in the cat's posterior auditory field. J Neurophysiol 79:3041–3059.

Hendry SHC, Jones EG. 1983. Thalamic inputs to identified commissural neurons in the monkey somatic sensory cortex. J Neurocytol 12:299–316.

Henke-Fahle S, Mann F, Götz M, Wild K, Bolz J. 1996. Dual action of a carbohydrate epitope on afferent and efferent axons in cortical development. J Neurosci 16:4195–4206.

Herkenham M. 1980. Laminar organization of thalamic projections to rat neocortex. Science 205:532–534.

Huang CL, Winer JA. 1997. Areal and laminar distribution of cat auditory thalamocortical projections. Proc Soc Neurosci 24:185.

Huang CL, Winer JA. 1998. Laminar patterns of auditory thalamocortical input in the cat: a quantitative approach. Proc Soc Neurosci 24:1881.

Huang CL, Larue DT, Winer JA. 1999. GABAergic organization of the cat medial geniculate body. J Comp Neurol 415:368–392.

Humphrey AL, Sur M, Uhlrich DJ, Sherman SM. 1985a. Projection patterns of individual X- and Y-cell axons from the lateral geniculate nucleus to cortical area 17 in the cat. J Comp Neurol 233:159–189.

Humphrey AL, Sur M, Uhlrich DJ, Sherman SM. 1985b. Termination patterns of individual X- and Y-cell axons in the visual cortex of the cat: Projections to area 18, to the 17/18 border region, and to both areas 17 and 18. J Comp Neurol 233:190–212.

Imig TJ, Adrián HO. 1977. Binaural columns in the primary auditory field (A1) of cat auditory cortex. Brain Res 138:241–257.

Imig TJ, Morel A. 1984. Topographic and cytoarchitectonic organization of thalamic neurons related to their targets in low-, middle-, and high-frequency representations in cat auditory cortex. J Comp Neurol 227: 511–539.

Imig TJ, Morel A. 1985. Tonotopic organization in ventral nucleus of medial geniculate body in the cat. J Neurophysiol 53:309–340.

Jensen KF, Killackey HP. 1987. Terminal arbors of axons projecting to the somatosensory cortex of the adult rat. II. The altered morphology of thalamocortical afferents following neonatal infraorbital nerve cut. J Neurosci 7:3544–3553.

Johnson RA. 1992. Applied multivariate statistical analysis. Englewood Cliffs, NJ: Prentice-Hall.

Jones, EG. 1975. Lamination and differential distribution of thalamic afferents within the sensory-motor cortex of the squirrel monkey. J Comp Neurol 160:167–204.

Jones EG. 1984. Organization of the thalamocortical complex and its relation to sensory processes. In: Darian-Smith I, editor. Handbook of physiology, section 1: the nervous system, vol III: sensory processes, part 1. Washington, DC: American Physiological Society. p 149–212.

Jones EG. 1985. The thalamus. New York: Plenum Press.

Jones EG, Burton H. 1974. Cytoarchitecture and somatic sensory connectivity of thalamic nuclei other than the ventrobasal complex in the cat. J Comp Neurol 154:395–432.

Jones EG, Burton H. 1976. Areal differences in the laminar distribution of thalamic afferents in cortical fields of the insular, parietal, and temporal regions of primates. J Comp Neurol 168:197–248.

Jones EG, Powell TPS. 1970. Electron microscopy of the somatic sensory cortex of the cat. Phil Trans R Soc (Lond) B 257:1–62.

Jones EG, Powell TPS. 1973. Anatomical organization of the somatosensory cortex. In: Iggo A, editor. Handbook of sensory physiology, vol II: somatosensory system. Berlin: Springer-Verlag. p 579–620.

Kelly JP, Wong D. 1981. Laminar connections of the cat's auditory cortex. Brain Res 212:1–15.

Kilgard MP, Merzenich MM. 1998. Cortical map reorganization enabled by nucleus basalis activity. Science 279:1714–1718.

Killackey HP, Ebner FF. 1972. Two different types of thalamocortical projections to a single cortical area in mammals. Brain Behav Evol 6:141–169.

Krubitzer L, Manger P, Pettigrew J, Calford M. 1995. Organization of somatosensory cortex in monotremes: in search of the prototypical plan. J Comp Neurol 351:261–306.

Landry P, Deschênes M. 1981. Intracortical arborizations and receptive fields of identified ventrobasal thalamocortical afferents to the primary somatic sensory cortex in the cat. J Comp Neurol 199:345–372.

Lane RD, Bennett-Clarke CA, Chiaia NL, Killackey HP, Rhoades RW. 1995. Lesion-induced reorganization in the brainstem is not completely expressed in somatosensory cortex. Proc Natl Acad Sci USA 92:4264–4268.

LeDoux JE, Iwata J, Pearl D, Reis DJ. 1986. Disruption of auditory but not visual learning by destruction of intrinsic neurons in the rat medial geniculate body. Brain Res 371:395–399.

Lende RA. 1963. Cerebral cortex: a sensorimotor amalgam in the Marsupialia. Science 141:730–732.

Lende RA, Sadler KM. 1967. Sensory and motor areas in neocortex of hedgehog (*Erinaceus*). Brain Res 5:390–405.

LeVay S, Gilbert CD. 1976. Laminar patterns of geniculocortical projection in the cat. Brain Res 113:1–19.

Leventhal AG. 1979. Evidence that the different classes of relay cells of the cat's lateral geniculate nucleus terminate in different layers of the striate cortex. Exp Brain Res 37:349–372.

Leventhal A, Rodieck RW, Dreher B. 1981. Retinal ganglion cell classes in the Old World monkey: morphology and central projections. Science 213:1139–1142.

Love JA, Scott JW. 1969. Some response characteristics of cells in the magnocellular division of the medial geniculate body of the cat. Can J Physiol Pharmacol 47:881–888.

Marín-Padilla M. 1984. Neurons of layer I. A developmental analysis. In: Peters A, Jones EG, editors. Cerebral cortex, vol 1: cellular components of the cerebral cortex. New York: Plenum Press. p 447–478.

Markram H, Wang Y, Tsodyks M. 1998. Differential signaling via the same axon of neocortical pyramidal neurons. Proc Natl Acad Sci USA 95: 5323–5328.

McAllister JP, Wells J. 1981. The structural organization of the ventral posterolateral nucleus in the rat. J Comp Neurol 197:271–301.

McMullen NT, de Venecia RK. 1993. Thalamocortical patches in auditory neocortex. Brain Res 620:317–322.

Merzenich MM, Knight PL, Roth GL. 1975. Representation of cochlea within primary auditory cortex in the cat. J Neurophysiol 38:231–249.

Mesulam M-M. 1978. Tetramethyl benzidine for horseradish peroxidase neurohistochemistry: a non-carcinogenic blue reaction-product with superior sensitivity for visualizing neural afferents and efferents. J Histochem Cytochem 26:106–117.

Mesulam M-M, Pandya DN. 1973. The projections of the medial geniculate complex within the Sylvian fissure of the rhesus monkey. Brain Res 60:315–333.

Metherate R, Ashe JH. 1995. Synaptic interactions involving acetylcholine, glutamate, and GABA in rat auditory cortex. Exp Brain Res 107:59–72.

Middlebrooks JC, Zook JM. 1983. Intrinsic organization of the cat's medial geniculate body identified by projections to binaural response-specific bands in the primary auditory cortex. J Neurosci 3:203–225.

Middlebrooks JC, Clock AE, Xu L, Green DM. 1994. A panoramic code for sound location by cortical neurons. Science 264:842–844.

Miller M. 1981. Maturation of rat visual cortex. I. A quantitative study of Golgi-impregnated pyramidal neurons. J Neurocytol 10:859–878.

Mitani A, Itoh K, Nomura S, Kudo M, Kaneko T, Mizuno N. 1984. Thalamocortical projections to layer I of the primary auditory cortex in the cat: a horseradish peroxidase study. Brain Res 310:347–350.

Mitani A, Itoh K, Mizuno N. 1987. Distribution and size of thalamic neurons projecting to layer I of the auditory cortical fields of the cat compared to those projecting to layer IV. J Comp Neurol 257:105–121.

Molnár Z, Blakemore C. 1991. Lack of regional specificity for connections formed between thalamus and cortex in coculture. Nature 351:475–477.

Morel A, Imig TJ. 1987. Thalamic projections to fields A, AI, P, and VP in the cat auditory cortex. J Comp Neurol 265:119–144.

Morest DK. 1964. The neuronal architecture of the medial geniculate body of the cat. J Anat (Lond) 98:611–630.

Morest DK. 1965. The laminar structure of the medial geniculate body of the cat. J Anat (Lond) 99:143–160.

Morest DK. 1975a. Structural organization of the auditory pathways. In: Tower DB, editor. The nervous system, vol. 3: human communication and its disorders. New York: Raven Press. p 19–29.

Morest DK. 1975b. Synaptic relationships of Golgi type II cells in the medial geniculate body of the cat. J Comp Neurol 162:157–194.

Neff WD, Diamond IT, Casseday JH. 1975. Behavioral studies of auditory discrimination: central nervous system. In: Keidel WD, Neff WD, editors. Handbook of sensory physiology, vol V, part 2: auditory system, anatomy, physiology (ear). Berlin: Springer-Verlag. p 307–400.

Niimi K, Matsuoka H. 1979. Thalamocortical organization of the auditory system in the cat studied by retrograde axonal transport of horseradish peroxidase. Adv Anat Embryol Cell Biol 57:1–56.

Niimi K, Naito F. 1972. Thalamo-cortical organization of the auditory system in the cat. Proc Jpn Acad Sci 48:619–624.

Niimi K, Naito F. 1974. Cortical projections of the medial geniculate body in the cat. Exp Brain Res 19:326–342.

Niimi K, Ono K, Kusunose M. 1984. Projections of the medial geniculate nucleus to layer 1 of the auditory cortex in the cat traced with horseradish peroxidase. Neurosci Lett 45:223–228.

Ogren MP, Hendrickson AE. 1979. The structural organization of the inferior and lateral subdivisions of the *Macaca* monkey pulvinar. J Comp Neurol 188:147–178.

O'Leary JL. 1940. A structural analysis of the lateral geniculate nucleus of the cat. J Comp Neurol 73:405–430.

Oliver DL, Hall WC. 1978. The medial geniculate body of the tree shrew, *Tupaia glis*. II. Connections with the neocortex. J Comp Neurol 182: 459–494.

Patterson HA. 1976. An anterograde degeneration and retrograde axonal transport study of the cortical projections of the rat medial geniculate body [thesis]. Boston: Department of Anatomy, Boston University Graduate School.

Penny GR, Itoh K, Diamond IT. 1982. Cells of different sizes in the ventral nuclei project to different layers of the somatic cortex in the cat. Brain Res 242:55–65.

Peters A, Feldman ML. 1977. The projection of the lateral geniculate nucleus to area 17 of the rat cerebral cortex. IV. Terminations upon spiny dendrites. J Neurocytol 6:669–689.

Peters A, Feldman M, Saldanha J. 1976. The projection of the lateral geniculate nucleus on area 17 of the rat cerebral cortex II terminations upon neuronal perikarya and dendritic shafts. J Neurocytol 5:85–107.

Popowits JM, Larue DT, Winer JA. 1988. Glutamate is a major transmitter in the rat medial geniculate body. Proc Soc Neurosci 14:490.

Prieto JJ, Winer JA. 1999. Neurons of layer VI in cat primary auditory cortex (AI): Golgi study and sublaminar origins of projection neurons. J Comp Neurol 404:332–358.

Prieto JJ, Peterson BA, Winer JA. 1994a. Morphology and spatial distribution of GABAergic neurons in cat primary auditory cortex (AI). J Comp Neurol 344:349–382.

Prieto JJ, Peterson BA, Winer JA. 1994b. Laminar distribution and neuronal targets of GABAergic axon terminals in cat primary auditory cortex (AI). J Comp Neurol 344:383–402.

Ramón y Cajal S. 1911. Histologie du système nerveux de l'homme et des vertébrés. Paris: Maloine [original French edition]. Madrid: Consejo Superior de Investigaciones Cientificas [1972].

Rausell E, Bickford L, Manger PR, Woods TM, Jones EG. 1998. Extensive divergence and convergence in the thalamocortical projection to monkey somatosensory cortex. J Neurosci 18:4216–4232.

Reale RA, Imig TJ. 1980. Tonotopic organization in auditory cortex of the cat. J Comp Neurol 182:265–291.

Rockland KS, Andresen J, Cowie RJ, Robinson DL. 1999. Single axon analysis of pulvinocortical connections to several visual areas in the macaque. J Comp Neurol 406:221–250.

Rose JE, Woolsey CN. 1949a. Organization of the mammalian thalamus and its relationships to the cerebral cortex. Electroenceph Clin Neurophysiol 1:391–404.

Rose JE, Woolsey CN. 1949b. The relations of thalamic connections, cellular structure, and evocable electrical activity in the auditory region of the cat. J Comp Neurol 91:441–466.

Rouiller EM, Rodrigues-Dagaeff C, Simm G, de Ribaupierre Y, Villa AEP, de Ribaupierre F. 1989. Functional organization of the medial division of the medial geniculate body of the cat: tonotopic organization, spatial distribution of response properties and cortical connections. Hear Res 39:127–146.

Rouiller EM, Simm GM, Villa AEP, de Ribaupierre Y, de Ribaupierre F. 1991. Auditory corticocortical interconnections in the cat: evidence for parallel and hierarchical arrangement of the auditory cortical areas. Exp Brain Res 86:483–505.

Ryugo DK, Killackey HP. 1974. Differential telencephalic projections of the medial and ventral divisions of the medial geniculate body of the rat. Brain Res 82:173–177.

Salt TE, Eaton SA. 1996. Functions of ionotropic and metabotropic glutamate receptors in sensory transmission in the mammalian thalamus. Progr Neurobiol 48:55–72.

Scheibel ME, Scheibel AB. 1966. Patterns of organization in specific and nonspecific thalamic fields. In: Purpura DP, Yahr MD, editors. The thalamus. New York: Columbia University Press. p 13–46.

Schreiner CE, Cynader MS. 1984. Basic functional organization of second auditory cortical field (AII) of the cat. J Neurophysiol 51:1284–1305.

Schreiner CE, Urbas JV. 1988. Representation of amplitude modulation in the auditory cortex of the cat. II. Comparison between cortical fields. Hear Res 32:49–64.

Shinonaga Y, Takada M, Mizuno N. 1994. Direct projections from the non-laminated divisions of the medial geniculate nucleus to the temporal polar cortex and amygdala in the cat. J Comp Neurol 340:405–426.

Society for Neuroscience. 1991. Handbook for the use of animals in neuroscience research. Washington, DC: Society for Neuroscience.

Sousa-Pinto A. 1973a. Cortical projections of the medial geniculate body in the cat. Adv Anat Embryol Cell Biol 48:1–42.

Sousa-Pinto A. 1973b. The structure of the first auditory cortex (A I) in the cat. I.—Light microscopic observations on its structure. Arch Ital Biol 111:112–137.

Sousa-Pinto A, Reis FF. 1975. Selective uptake of [^{3}H]leucine by projection neurons of the cat auditory cortex. Brain Res 85:331–336.

Sousa-Pinto AA, Paula-Barbosa MM, Matos MDC. 1975. A Golgi and electron microscopical study of nerve cells in layer I of the cat auditory cortex. Brain Res 95:443–458.

Spreafico R, De Biasi S, Battaglia G, Rustioni A. 1992. GABA- and glutamate-containing neurons in the thalamus of rats and cats: an immunocytochemical study. Epilepsy Res 8(Suppl):107–115.

Steriade M. 1997. Thalamic substrates and disturbances in states of vigilance and consciousness in humans. In: Steriade M, Jones EG, McCormick DA, editors. Thalamus, vol II: experimental and clinical aspects. Amsterdam: Elsevier Science. p 721–742.

Steriade M, Jones EG, McCormick DA. 1997. Thalamus, vol I: organisation and function. Amsterdam: Elsevier Science Ltd.

Symonds LL, Rosenquist AC, Edwards SB, Palmer LA. 1981. Projections of the pulvinar-lateral posterior complex to visual cortical areas in the cat. Neuroscience 6:1995–2020.

Tusa RJ, Palmer LA, Rosenquist AC. 1978. The retinotopic organization of area 17 (striate cortex) in the cat. J Comp Neurol 177:213–236.

Uhlrich D, Huguenard JR. 1995. Purinergic inhibition of GABA and glutamate release in the thalamus: implications for thalamic network activity. Neuron 15:909–918.

Wall JT. 1988. Development and maintenance of somatotopic maps of the skin: a mosaic hypothesis based on peripheral and central contiguities. Brain Behav Evol 31:252–268.

Weinberger NM, Diamond DM. 1987. Physiological plasticity in auditory cortex: rapid induction by learning. Prog Neurobiol 29:1–55.

Wepsic JG. 1966. Multimodal sensory activation of cells in the magnocellular medial geniculate nucleus. Exp Neurol 15:299–318.

White EL, Keller A. 1989. Cortical circuits. Synaptic organization of the cerebral cortex. Structure, function, and theory. Boston: Birkhäuser.

Wilson ME, Cragg BG. 1969. Projections from the medial geniculate body to the cerebral cortex in the cat. Brain Res 13:462–475.

Winer JA. 1984a. Anatomy of layer IV in cat primary auditory cortex (AI). J Comp Neurol 224:535–567.

Winer JA. 1984b. The non-pyramidal neurons in layer III of cat primary auditory cortex (AI). J Comp Neurol 229:512–530.

Winer JA. 1984c. The pyramidal cells in layer III of cat primary auditory cortex (AI). J Comp Neurol 229:476–496.

Winer JA. 1985a. The medial geniculate body of the cat. Adv Anat Embryol Cell Biol 86:1–98.

Winer JA. 1985b. Structure of layer II in cat primary auditory cortex (AI). J Comp Neurol 238:10–37.

Winer JA. 1992. The functional architecture of the medial geniculate body and the primary auditory cortex. In: Webster DB, Popper AN, Fay RR, editors. Springer handbook of auditory research, vol 1: the mammalian auditory pathway: neuroanatomy. New York: Springer-Verlag. p 222–409.

Winer JA, Larue DT. 1987. Patterns of reciprocity in auditory thalamocortical and corticothalamic connections: study with horseradish peroxidase and autoradiographic methods in the rat medial geniculate body. J Comp Neurol 257:282–315.

Winer JA, Larue DT. 1988. Anatomy of glutamic acid decarboxylase (GAD) immunoreactive neurons and axons in the rat medial geniculate body. J Comp Neurol 278:47–68.

Winer JA, Larue DT. 1989. Populations of GABAergic neurons and axons in layer I of rat auditory cortex. Neuroscience 33:499–515.

Winer JA, Morest DK. 1983a. The medial division of the medial geniculate body of the cat: implications for thalamic organization. J Neurosci 3:2629–2651.

Winer JA, Morest DK. 1983b. The neuronal architecture of the dorsal division of the medial geniculate body of the cat. A study with the rapid Golgi method. J Comp Neurol 221:1–30.

Winer JA, Morest DK. 1984. Axons of the dorsal division of the medial geniculate body of the cat: a study with the rapid Golgi method. J Comp Neurol 224:344–370.

Winer JA, Wenstrup JJ. 1994. The neurons of the medial geniculate body in the mustached bat (*Pteronotus parnellii*). J Comp Neurol 346:183–206.

Winer JA, Larue DT, Diehl JJ, Hefti BJ. 1998. Auditory cortical projections to the cat inferior colliculus. J Comp Neurol 400:147–174.

Winguth SD, Winer JA. 1986. Corticocortical connections of cat primary auditory cortex (AI): laminar organization and identification of supragranular neurons projecting to area AII. J Comp Neurol 248:36–56.

Woolsey CN, editor. 1981a. Cortical sensory organization, vol 1: multiple somatic areas. Humana Press, Clifton, NJ.

Woolsey CN, editor. 1981b. Cortical sensory organization, vol 2: multiple visual areas. Humana Press, Clifton, NJ.

Woolsey CN, editor. 1982. Cortical sensory organization, vol 3: multiple auditory areas. Clifton, NJ: Humana Press.